Elements of Photonics, Volume II: For Fiber and Integrated Optics. Keigo Iizuka

ISBNs: 0-471-40815-8 (Hardback); 0-471-22137-6 (Electronic)

9

PLANAR OPTICAL GUIDES FOR INTEGRATED OPTICS

The contents of Chapters 9 and 10 are closely interwoven. Both chapters deal with guided waves, but Chapter 9 deals primarily with guided waves in a medium bounded in one direction (taken as the x direction), while Chapter 10 deals with guided waves in a medium bounded in two directions (taken as the x and y directions). The slab optical guide is an example of a medium bounded in one direction; and the rectangular optical guide is an example of a medium bounded in two directions. For the analysis in both Chapters 9 and 10, the z direction is taken as the direction of the wave propagation.

The foundation of integrated optics is the planar optical guide. The light is guided by a medium whose index of refraction is higher than that of surrounding layers. An optical guide made of an electrooptic material changes its characteristics with a change in the applied electric field. This type of guide is very useful for fabricating electronically controllable optical switches, directional couplers, interferometers, and modulators.

According to geometrical optics, light will propagate by successive total internal reflections with very little loss provided that certain conditions are met. These conditions are that the layer supporting the propagation must have a higher refractive index than the surrounding media, and the light must be launched within an angle that satisfies total internal reflection at the upper and lower boundaries. This simple geometrical optics theory fails when the dimensions of the guiding medium are comparable to the wavelength of the light. In this regime, the guide supports propagation only for a discrete number of angles, called *modes of propagation*. In this chapter, the concept of modes of propagation is fully explored. We will explain what a mode looks like, how many modes there are, how to suppress some unwanted modes, and how to accentuate only one particular mode. This information is essential for designing an optical guide.

The chapter starts with the characteristic equation that primarily controls the mode configuration. Then, details of each mode are described. Due to the simplicity of the geometries studied, exact solutions will be obtained in many cases. Such knowledge is essential for designing the various optical waveguide configurations in the next chapter.

9.1 CLASSIFICATION OF THE MATHEMATICAL APPROACHES TO THE SLAB OPTICAL GUIDE

Slab optical guides consist of three planes and can broadly be classed into two types. One is the symmetric guide and the other is the asymmetric guide. "Slab optical guide" will be called simply "guide." The refractive indices of the top and bottom layers of the symmetric guide are identical, as indicated in Fig. 9.1, whereas those of an asymmetric guide are different. In integrated optics, both types are used. The core material of the symmetric guide is completely imbedded inside the substrate (cladding) material. The asymmetric guide consists of a film layer as the guiding core layer, with air or some other covering material as the top cladding layer, and substrate as the bottom cladding layer.

Since the mathematics dealing with a symmetric guide is much simpler than that of an asymmetric guide, the symmetric guide will be treated first for better physical insight.

The commonly used methods of analysis are the following:

1. The wave optics approach, which is the most rigorous but sometimes more complicated method.
2. The coefficient matrix approach whose manipulation is more or less mechanical and straightforward.
3. The transmission matrix method, which has the potential to be extended to solve multilayer problems.
4. The modified ray model method, which is simple but provides less information.

The wave optics approach is explained in Sections 9.2 to 9.6 and the other methods in Section 9.7.

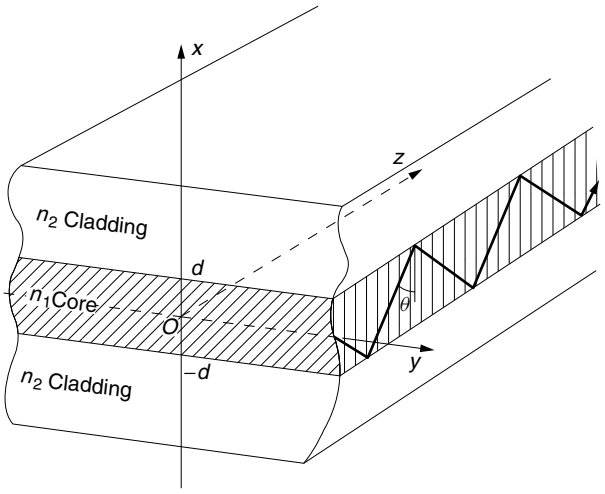

Figure 9.1 Geometry of the slab optical guide.

9.2 WAVE OPTICS APPROACH

This method starts with Maxwell's equations [1–5]. It needs no approximation and the results are rigorous. First, the field expressions are derived, followed by a derivation of the characteristic equations that are instrumental in determining the propagation modes in the guide.

Let a sinusoidally time-varying wave propagate in the z direction. The propagation constant in the z direction is β. The electric and magnetic components of the wave are expressed as

$$\begin{aligned} \mathbf{E} &= \mathbf{E}_0(x, y)e^{j(\beta z-\omega t)} \\ \mathbf{H} &= \mathbf{H}_0(x, y)e^{j(\beta z-\omega t)} \end{aligned} \tag{9.1}$$

The following two assumptions simplify the analysis:

Assumption 1. No component of the field varies in the y direction:

$$\frac{\partial}{\partial y} = 0 \tag{9.2}$$

Assumption 2. There is no magnetic field component in the z direction (TM modes),

$$H_z = 0 \tag{9.3}$$

The first assumption means that a wave is launched that does not vary in the y direction. This means that the field extends indefinitely in the y direction, but in reality there is no such wave. Note also that an infinite dimension does not guarantee Assumption 1. The infinity of the y dimension of the layer is certainly a necessary condition for $\partial/\partial y = 0$, but not a sufficient condition. For instance, a plane wave has variations even in an infinitely large medium in the direction of propagation. The manner of launching determines this condition.

The second assumption leads to a natural way of dividing the solutions, but it is not the only way to divide the solutions. The solutions are separated into two waves: one that has only transverse and no longitudinal magnetic field, that is, $H_z = 0$; and the other that has only transverse and no longitudinal electric field, that is, $E_z = 0$. The former is called *transverse magnetic* or TM mode (wave) and the latter, a *transverse electric* or TE mode. In general, a wave has both H_z and E_z components. The H_z component is accounted for by the H_z component of the TE mode and the E_z component, by the E_z component of the TM mode. The field is composed of both TM and TE modes in general. Except for Section 9.6, TM modes are assumed in this chapter.

With the assumption of Eq. (9.2), the H_y component of Eq. (9.1) is found first by inserting it into the wave equation:

$$\nabla^2\mathbf{H} + (n_{1,2}k)^2\mathbf{H} = 0 \tag{9.4}$$

$$\frac{\partial^2 H_y}{\partial x^2} + (n_{1,2}^2k^2 - \beta^2)H_y = 0 \tag{9.5}$$

Equation (9.5) is applicable for both core and cladding layers by using the respective values of n_1 or n_2 for $n_{1,2}$.

There are two kinds of solutions for the differential equation, Eq. (9.5): trigonometric solutions such as $\cos Kx$ or $\sin Kx$ for a positive value of $(n_{1,2}^2 k^2 - \beta^2)$, and exponential solutions such as $e^{\gamma x}$ or $e^{-\gamma x}$ for a negative value of $(n_{1,2}^2 k^2 - \beta^2)$. Here, only the guided wave is treated, that is, the wave whose amplitude decays with both x and $-x$. The solutions are chosen to fit the physical conditions of the guided wave. Inside the core layer, the wave is oscillatory and the trigonometric solutions are suitable. Inside the cladding layer, however, only the evanescent wave is allowed and the solution must have a decaying nature. Thus, inside the core one has

$$n_1^2 k^2 - \beta^2 = K^2 \quad |x| < d \tag{9.6}$$

and in the cladding,

$$n_2^2 k^2 - \beta^2 = -\gamma^2 \quad |x| > d \tag{9.7}$$

The range of values of β^2 that satisfy both Eqs. (9.6) and (9.7) is limited. The left-hand side of Eq. (9.6) has to be positive, while that of Eq. (9.7) has to be negative. This is especially true because the difference between n_1 and n_2 is normally a fraction of 1% of n_1. The range of β set by Eqs. (9.6) and (9.7) is

$$n_1 k > \beta > n_2 k \tag{9.8}$$

Moreover, β is allowed to take only discrete values in the above range, as will be shown later.

The solution of Eq. (9.5) with Eq. (9.6) inside the core is

$$H_y = A \cos Kx + B \sin Kx \tag{9.9}$$

and the solution of Eq. (9.5) with Eq. (9.7) inside the cladding layer is

$$H_y = Ce^{-\gamma x} + De^{\gamma x} \tag{9.10}$$

where the factor $e^{j(\beta z - \omega t)}$ was suppressed.

The next step is to find the constants A, B, C, and D using the boundary conditions. In the upper cladding layer, D has to be zero (note that zero is also a legitimate constant) so as to prevent H_y from becoming infinitely large as x approaches $+\infty$. Using the same reasoning, C has to be zero in the lower cladding layer.

$$H_y = \begin{cases} Ce^{-\gamma x}, & x > d \\ De^{\gamma x}, & x < -d \end{cases} \tag{9.11}$$

Matters are simplified if Eq. (9.9) is separated into two parts:

$$H_y = A \cos Kx \tag{9.12}$$

$$H_y = B \sin Kx \tag{9.13}$$

In the end, the two solutions are combined to reach the final solution. Equation (9.12) is called the *even-mode solution*, and Eq. (9.13) is the *odd-mode solution*, simply because $\cos Kx$ is an even function of x (i.e., $\cos(-Kx) = \cos Kx$), and $\sin Kx$ is an odd function of x (i.e., $\sin(-Kx) = -\sin Kx$). This way of separating the solutions into

two is quite natural. If the slab optical guide is excited with an incident wave whose amplitude distribution is symmetric with respect to x, A is nonzero and B is zero. B is nonzero and A is zero for a perfectly antisymmetric incident amplitude distribution.

In order to determine the values of the constants, the boundary condition of the continuity of the tangential **H** field is used at $x = d$, and from Eqs. (9.11) and (9.12), this boundary condition for the even TM modes gives

$$A \cos Kd = Ce^{-\gamma d} \tag{9.14}$$

Putting this equation back into Eq. (9.11) gives

$$H_y = A(\cos Kd)e^{-\gamma(x-d)} \tag{9.15}$$

An expression for the lower cladding layer is obtained using the boundary condition at $x = -d$. The results for the even TM modes are summarized as

$$H_y = \begin{cases} A(\cos Kd)e^{-\gamma(x-d)} & \text{in the upper cladding} \\ A \cos Kx & \text{in the core} \\ A(\cos Kd)e^{\gamma(x+d)} & \text{in the lower cladding} \end{cases} \tag{9.16}$$

Expressions for the odd modes are obtained by starting with Eq. (9.13) instead of Eq. (9.12) and following the same procedure. The results for the odd TM modes are summarized as

$$H_y = \begin{cases} B(\sin Kd)e^{-\gamma(x-d)} & \text{in the upper cladding} \\ B \sin Kx & \text{in the core} \\ -B(\sin Kd)e^{\gamma(x+d)} & \text{in the lower cladding} \end{cases} \tag{9.17}$$

Next, E_x and E_z are obtained from H_y using Maxwell's equations:

$$\nabla \times \mathbf{H} = \frac{\partial \mathbf{D}}{\partial t} \tag{9.18}$$

$$\nabla \times \mathbf{E} = -\frac{\partial \mathbf{B}}{\partial t} \tag{9.19}$$

With Eqs. (9.1), (9.2), and (9.18), E_x and E_z are

$$E_x = \frac{\beta}{\omega \epsilon_r \epsilon_0} H_y \tag{9.20}$$

$$E_z = \frac{j}{\omega \epsilon_r \epsilon_0} \frac{\partial H_y}{\partial x} \tag{9.21}$$

The value of ϵ_r depends on the medium and

$$\epsilon_r = \begin{cases} n_1^2 & \text{in the core} \\ n_2^2 & \text{in the cladding} \end{cases} \tag{9.22}$$

Now, all field components of the TM modes have been obtained. They are summarized as

$$\begin{aligned} E_x &= \frac{\beta}{\omega\epsilon_r\epsilon_0} H_y \\ E_y &= 0 \\ E_z &= \frac{j}{\omega\epsilon_r\epsilon_0}\frac{\partial H_y}{\partial x} \\ H_x &= 0 \\ H_y &= A\cos Kx + B\sin Kx \\ H_z &= 0 \end{aligned} \tag{9.23}$$

where $B = 0$ for the even TM modes, and $A = 0$ for the odd TM modes. The equation $E_y = 0$ was derived from Maxwell's equations as follows. The y component of Eq. (9.18) and the x component of Eq. (9.19) are combined to give

$$E_y(\omega^2\mu\epsilon_r\epsilon_0 - \beta^2) = 0 \tag{9.24}$$

Since the value inside the parentheses is K^2 from Eq. (9.6) and is nonzero, $E_y = 0$. $H_x = 0$ was derived by inserting $E_y = 0$ into the x component of Eq. (9.19).

9.3 CHARACTERISTIC EQUATIONS OF THE TM MODES

In the previous section, not much was said about the actual values of K^2 and $-\gamma^2$ except that the former is a positive number and the latter, a negative number. The values of K and γ are crucial to determining the modes of propagation. Some more boundary conditions are used to find these values.

9.3.1 Solutions for K and γ

First, the even TM modes are considered. Continuity of the tangential $\mathbf{E}$ field, E_z in Eq. (9.23), at $x = d$ requires that

$$n^2 AK\sin Kd = \gamma C e^{-\gamma d} \tag{9.25}$$

where Eqs. (9.11), (9.12), and (9.21) and $n = \sqrt{\epsilon_{r2}/\epsilon_{r1}} = n_2/n_1$ were used. Dividing Eq. (9.25) by Eq. (9.14) gives

$$n^2 Kd\tan Kd = \gamma d \tag{9.26}$$

Equation (9.26) is called the *characteristic equation* for the even TM modes. The characteristic equation is used to find the solutions for K and γ.

We need one more equation to find the values of K and γ. From Eqs. (9.6) and (9.7), β is eliminated to obtain

$$(Kd)^2 + (\gamma d)^2 = V^2 \tag{9.27}$$

where

$$V = kd\sqrt{n_1^2 - n_2^2} \tag{9.28}$$

Since V consists of only physical constants such as the height of the guide, the indices of refraction, and the light wavelength, V is referred to as the *normalized thickness of the guide*. The normalized thickness V is an important parameter specifying the characteristics of the guide.

Equations (9.26) and (9.27) are transcendental equations and the solution cannot be found in a closed form. Graphical solutions are available, as shown in Fig. 9.2. Equations (9.26) and (9.27) are plotted on the Kd–γd plane as solid lines in Fig. 9.2. Note that Eq. (9.27) is a circle with radius V. The shape of the curve for Eq. (9.26) is quite similar to tan Kd. Each intersection point shown in Fig. 9.2 corresponds to a solution, or mode of propagation, of an even TM mode. These intersections are called, for short, the even TM modes.

The corresponding characteristic equation for the odd TM modes is obtained using Eq. (9.13) instead of Eq. (9.12). The continuity of H_y at $x = d$ gives

$$B \sin Kd = Ce^{-\gamma d} \tag{9.29}$$

and the continuity of E_z in Eq. (9.23) gives

$$n^2 BK \cos Kd = -C\gamma e^{-\gamma d} \tag{9.30}$$

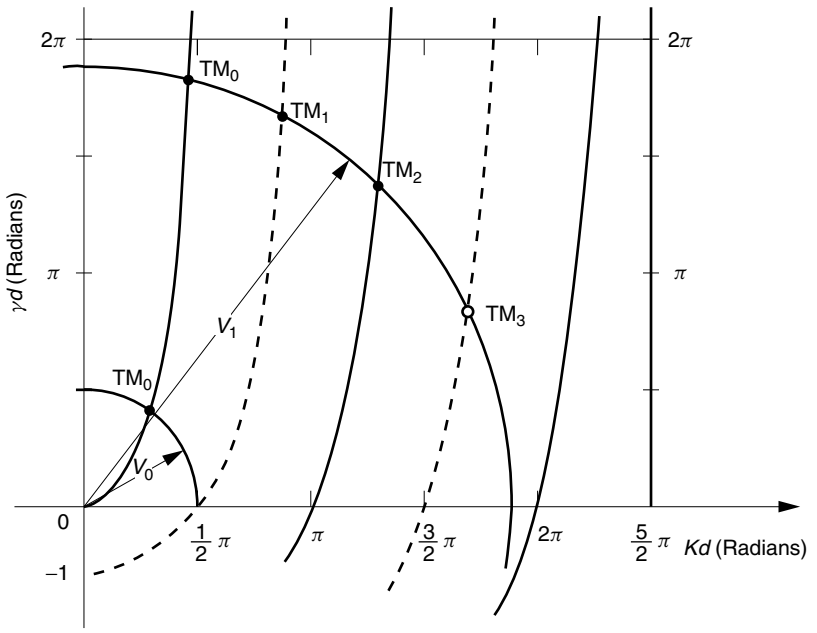

Figure 9.2 Graphical solutions for the even TM modes ($\gamma d = n^2 Kd \tan Kd$) in solid lines, and odd TM modes ($-\gamma d = n^2 Kd \cot Kd$) in dashed lines. $V = kd\sqrt{n_1^2 - n_2^2}$.

Division of Eq. (9.30) by Eq. (9.29) renders the characteristic equation for the odd TM modes as

$$-n^2 Kd \cot Kd = \gamma d \tag{9.31}$$

Equation (9.31) is plotted as the dashed lines in Fig. 9.2.

The intersections between the solid lines and the circle are the even (order) TM modes and those between the dashed lines and the circle are the odd (order) TM modes. Even numbered subscripts are used for even modes and odd numbers for odd modes. The subscript is called the *order of the mode* or the *mode number*.

With a decrease in V, the number of modes that the guide can support decreases one by one. For example, referring to Fig. 9.2, an optical guide whose normalized thickness is V_1 can support four modes, whereas that with V_0 can support only one mode. For every $\pi/2$-radian decrease in V, even and odd modes alternately disappear. The disappearance of a particular mode is called the *cutoff* of that mode. For instance, the cutoff condition for the TM_3 mode is $V = \frac{3}{2}\pi$. As the cutoff condition is approached, the value of γ approaches zero, and the effective depth of the evanescent wave (Section 2.8) in the cladding layer increases. When γ reaches zero, the evanescent wave is present throughout the cladding layer and the light energy cannot be sustained inside the core.

As long as V is greater than $\pi/2$, more than one mode can be excited simultaneously. Among the excited modes, the higher order modes are more susceptible to the conditions outside the guide because γ is smaller and the effective depth of the evanescent wave is deeper.

If V is less than $\pi/2$, there exists only one mode and no other modes can be excited. The mode that is capable of being the only excited mode is called the *dominant mode*. The dominant mode of the TM modes in the slab optical guide is the TM_0 mode. Note also that there is no cutoff for the TM_0 mode, which remains excited down to $V = 0$.

A slab optical guide that exclusively supports the dominant mode is called a single-mode guide or monomode guide. Guides that support more than one mode are called multimode guides. When light is launched into a multimode guide such that several modes are excited, then the incident light power is divided among the excited modes. Each mode, however, has a different propagation constant β_N. Thus, each mode arrives at the receiving point at a different phase and the signal is distorted. This distortion is called *mode dispersion*. A signal in a monomode guide is not distorted by mode dispersion.

Since the number of modes increases for every $\pi/2$-radian increase in V, the highest mode number N is the largest integer that still satisfies

$$\frac{2\pi}{\lambda} d \sqrt{n_1^2 - n_2^2} > N \frac{\pi}{2} \tag{9.32}$$

and the total number of TM modes including the zero-order mode is $N + 1$.

9.3.2 Examples Involving TM Modes

Example 9.1 Optical communication systems are normally operated at a light wavelength of 0.85, 1.3, or 1.55 μm. These wavelengths are outside the visible range. A

He–Ne laser emitting light at 0.63 μm is often used to test devices because 0.63 μm lies in the visible wavelength range.

A symmetric guide designed to be monomode for a wavelength of 1.3 μm was excited by a He–Ne laser. At most, how many TM modes will be excited by the He–Ne laser in this guide?

Solution According to Fig. 9.2, the largest normalized thickness V of a single-mode guide is $\pi/2$. Setting $V = \pi/2$ at 1.3 μm, the thickness d of such a guide is

$$\frac{2\pi}{1.3} d\sqrt{n_1^2 - n_2^2} = \frac{\pi}{2}$$

With this d, for 0.63 μm, the normalized thickness becomes

$$\begin{aligned} V &= \frac{2\pi}{0.63} d\sqrt{n_1^2 - n_2^2} \\ &= \frac{\pi}{2} \cdot \frac{1.3}{0.63} \\ &= 1.03\pi \text{ radians} \end{aligned}$$

From Fig. 9.2, at most three modes are excited. □

Example 9.2 The TM_2 mode in a symmetric guide was observed to be cut off when the wavelength was increased beyond 1.5 μm. The refractive index of the core is $n_1 = 1.55$ and that of the cladding is $n_2 = 1.54$.

(a) What is the thickness $2d$ of the guide?
(b) What is K_2 at the cutoff?
(c) What is β_2 at the cutoff?

The subscripts on K and β refer to the mode number.

Solution

(a) From Fig. 9.2, the TM_2 mode has its cutoff at $V = \pi$.

$$\frac{2\pi}{\lambda} d\sqrt{n_1^2 - n_2^2} = \pi$$

$$2d = \frac{\lambda}{\sqrt{n_1^2 - n_2^2}} = \frac{1.5}{\sqrt{1.55^2 - 1.54^2}} = 8.53 \text{ μm}$$

(b) At the cutoff, the normalized thickness is

$$V = K_2 d = \pi$$

and the value of K_2 is

$$K_2 = 0.74 \text{ rad/μm}$$

(c) At the cutoff, $\gamma_2 = 0$. Putting $\gamma_2 = 0$ in Eq. (9.7), one finds that β_c at the cutoff is $n_2 k$:

$$\beta_c = 6.4 \text{ rad}/\mu\text{m}$$

This relationship can also be derived from Eq. (9.6). Expressing Eq. (9.6) in terms of β_2 gives

$$\beta_2 = \sqrt{(n_1 k)^2 - K_2^2}$$

At the cutoff, $V = K_2 d$ and

$$K_2^2 = k^2(n_1^2 - n_2^2)$$

Inserting this K_2^2 value into the equation for β_2 gives β_c at the cutoff:

$$\beta_c = n_2 k$$

It is interesting to note that at the cutoff, the propagation constant is $n_2 k$ regardless of the order of the mode. □

Example 9.3 Show that if the slab guide can be excited up to the $(N_{\max})$th $\text{TM}_{N_{\max}}$ mode, the propagation constant β_N for the Nth ($N \ll N_{\max}$) TM_N mode can be approximated as

$$\beta_N = n_1 k \sqrt{1 - 2\Delta \left(\frac{N+1}{N_{\max}}\right)^2}$$

where

$$\Delta = \frac{n_1 - n_2}{n_1} \ll 1$$

$$N \ll N_{\max}$$

Solution The propagation constant β_N for the Nth TM mode is, from Eq. (9.6),

$$\beta_N = n_1 k \sqrt{1 - \left(\frac{K_N}{n_1 k}\right)^2} \tag{9.33}$$

The values of K_N in the region of

$$N \ll N_{\max}$$

are, from Fig. 9.2,

$$K_N d = \frac{\pi}{2}(N+1) \tag{9.34}$$

The missing information is d. The order of the highest mode is $N_{\max}$ and the corresponding V is

$$V = \frac{\pi}{2} N_{\max} \tag{9.35}$$

From Eq. (9.28) and the condition imposed on Δ, V can be expressed as

$$V = n_1 kd\sqrt{2\Delta} \tag{9.36}$$

Inserting the value of d obtained from Eqs. (9.35) and (9.36) into Eq. (9.34) gives the value for K_N. The final result is obtained by inserting this K_N value into Eq. (9.33), giving

$$\beta_N = n_1 k\sqrt{1 - 2\Delta\left(\frac{N+1}{N_{\max}}\right)^2} \tag{9.37}$$

□

9.4 CROSS-SECTIONAL DISTRIBUTION OF LIGHT AND ITS DECOMPOSITION INTO COMPONENT PLANE WAVES

The cross-sectional distribution of light in the guide is given by Eq. (9.16) or (9.17) and is shown in Fig. 9.3. The intensity distribution of the Nth-order TM mode has $N + 1$ loops and N nulls in the core layer. The shapes of the curves in Fig. 9.3 are determined by the value of K. If the even-mode K_N are far from the cutoff and are almost an odd multiple of $\pi/2$, then the field vanishes at $x = d$; but if the values of K_N for the even modes are smaller than an odd multiple of $\pi/2$, then the field at $x = d$ becomes a finite value. In fact, these finite values determine the amplitude of the evanescent field in the cladding layer.

It will be shown that the mode patterns are nothing but the standing-wave pattern produced by the interference of component plane waves zigzagging inside the optical guide. If the trigonometric cosine function is rewritten in exponential functions, Eq. (9.12) combined with Eq. (9.1) becomes

$$H_y = \tfrac{1}{2}A(e^{j(Kx+\beta z-\omega t)} + e^{j(-Kx+\beta z-\omega t)}) \tag{9.38}$$

Note from Chapter 1 that a plane wave propagating in the $\mathbf{k} = (k_x, k_y, k_z)$ direction is expressed by

$$e^{j\mathbf{k}\cdot\mathbf{r}} = e^{jk_x x + jk_y y + jk_z z}$$

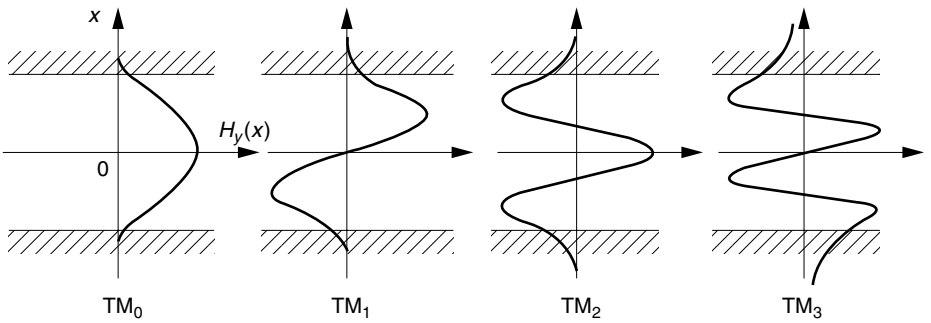

Figure 9.3 Distribution of the H_y field in the slab optical guide. The field distributions correspond to the modes in Fig. 9.2.

The first term of Eq. (9.38) is a component plane wave propagating slightly upward in the direction connecting the origin and a point (K, β) in the $x-z$ plane. The second term is a similar plane wave but propagating slightly downward in the direction connecting the origin and a point $(-K, \beta)$ in the same plane.

The interference of these two component plane waves is nothing but the field distribution of the mode. The spacing between adjacent null contour lines changes as the angle between the two plane waves is changed. This behavior can be demonstrated by drawing phase lines on two sheets of transparent paper, and then placing one over the top of the other as shown in Fig. 9.4. The phasefronts of these plane waves are designated by two kinds of lines. The 0° phase line is represented by a heavy line and the 180° phase line is represented by a fine line. The intersections of two heavy lines are the points of maximum amplitude, while the intersections of two fine lines are the points of minimum amplitude (negative extrema). The location where a fine line meets a heavy line indicates a null amplitude. The contours of the amplitude extrema and amplitude nulls are lines parallel to the z axis and alternate. The cross-sectional distribution along the x axis would look like the sinusoidal curve indicated on the right-hand side of Fig. 9.4. This sinusoidal curve is nothing but the mode pattern in the guide.

The spacing between the null amplitude contour lines starts to contract from the maximum of infinite distance to one-half wavelength by rotating from the parallel position to the perpendicular position. The angles between the component waves that can match the boundary condition are found by adjusting the rotation of the sheet. The boundary condition is met by lining up the null contours close to the upper and lower boundaries of the guide (to be exact, slightly inside the cladding layer due to the evanescent wave). For a given value $2d$ of the guide, the boundary conditions are

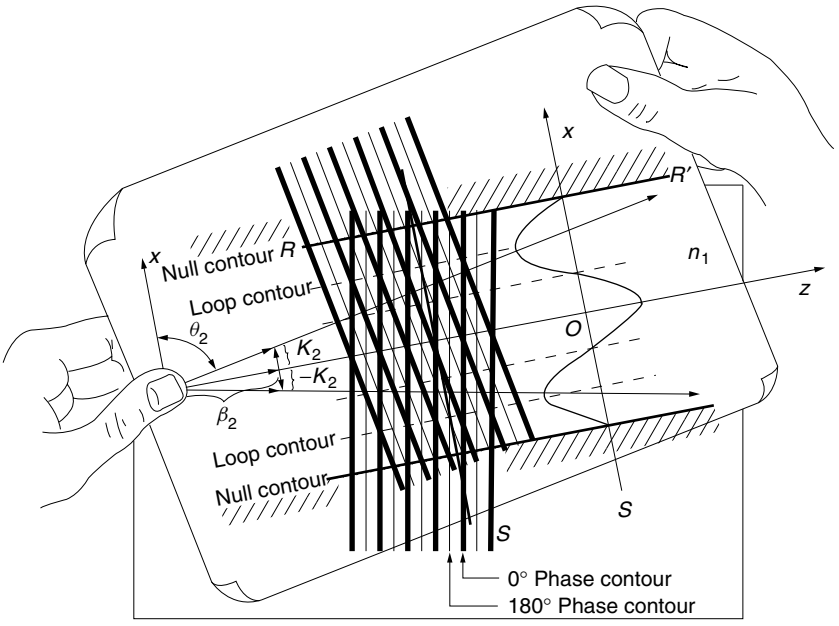

Figure 9.4 Composition of the TM_2 mode in terms of component plane waves. The effective index of refraction is $N = n_1 \sin\theta_2$.

satisfied only for a discrete number of angles θ_N. Conversely, for a given angle θ_1, the values of $2d$ that satisfy the boundary condition are discrete.

Because the field does not become exactly null on the boundary but goes into the cladding layer as an evanescent wave, there is some inaccuracy in situating the null contour line by this method. This inaccuracy can be removed by finding the value of K from Fig. 9.2 and then using Eq. (9.6) to find β and hence the angle θ_N. In this way, the directions of propagation that satisfy the boundary conditions are accurately determined.

The relationship between K and β in Eq. (9.6) is graphically represented by the K–β circle of $K^2 + \beta^2 = (n_1 k)^2$ as shown in Fig. 9.5. By using K from Fig. 9.2, β is found from Fig. 9.5. The direction of propagation is a vector connecting the point (K, β) and the origin, as shown in Fig. 9.5. The extensions of these vectors determine the directions of the component waves in the guide, shown on the right-hand side. The discrete angles θ_N of propagation are, from Fig. 9.5,

$$\theta_N = \sin^{-1}\left(\frac{\beta_N}{n_1 k}\right) \tag{9.39}$$

The range of allowed values of β is limited. The maximum value of β is $n_1 k$ from Fig. 9.5. The minimum value of β is determined by the critical angle θ_c associated with the boundary between the core and cladding layer as

$$\theta_c = \sin^{-1}\left(\frac{n_2}{n_1}\right) \tag{9.40}$$

From Eqs. (9.39) and (9.40), the minimum value of β is $n_2 k$. The allowed range of β agrees with the earlier results of Eq. (9.8). The prohibited region is to the left of the $n_2 k$ line in Fig. 9.5. In a typical glass guide, $n_2/n_1 = 1.54/1.55$ and $\theta_c = 83.5°$. The allowed range is quite small, only 6.5°.

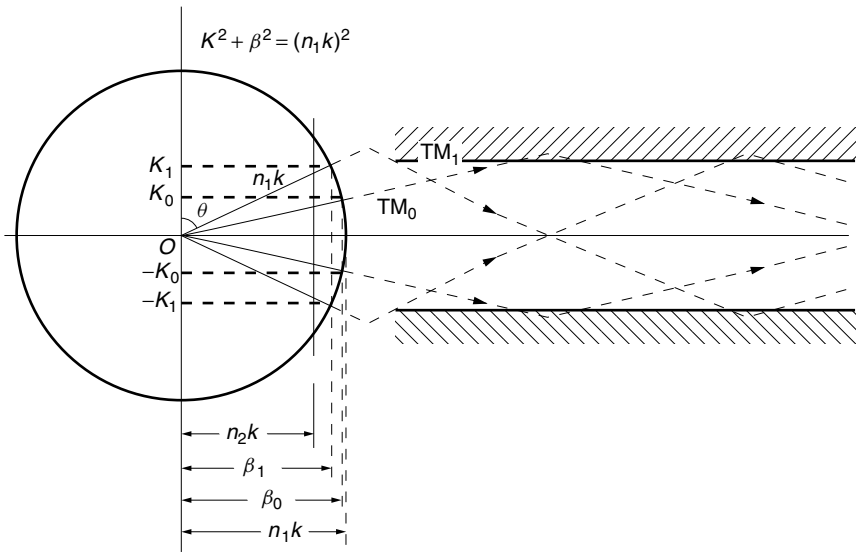

Figure 9.5 K–β circle and component waves.

Example 9.4 Using the TM_2 mode as an example, describe how the following quantities change as the thickness $2d$ of an optical guide is decreased: (a) K_2, (b) the incident angle θ_2 to the core–cladding interface, and (c) the cross-sectional field distribution of H_y.

Solution Figure 9.6 summarizes the results.

(a) The value of Kd is determined by the length p_2 shown in Fig. 9.6a:

$$K_2 = \frac{p_2}{d} \tag{9.41}$$

With a decrease in d, the value of $V = kd\sqrt{n_1^2 - n_2^2}$ decreases and hence p_2 decreases. With a decrease in d, both the numerator and denominator of Eq. (9.41) decrease. But

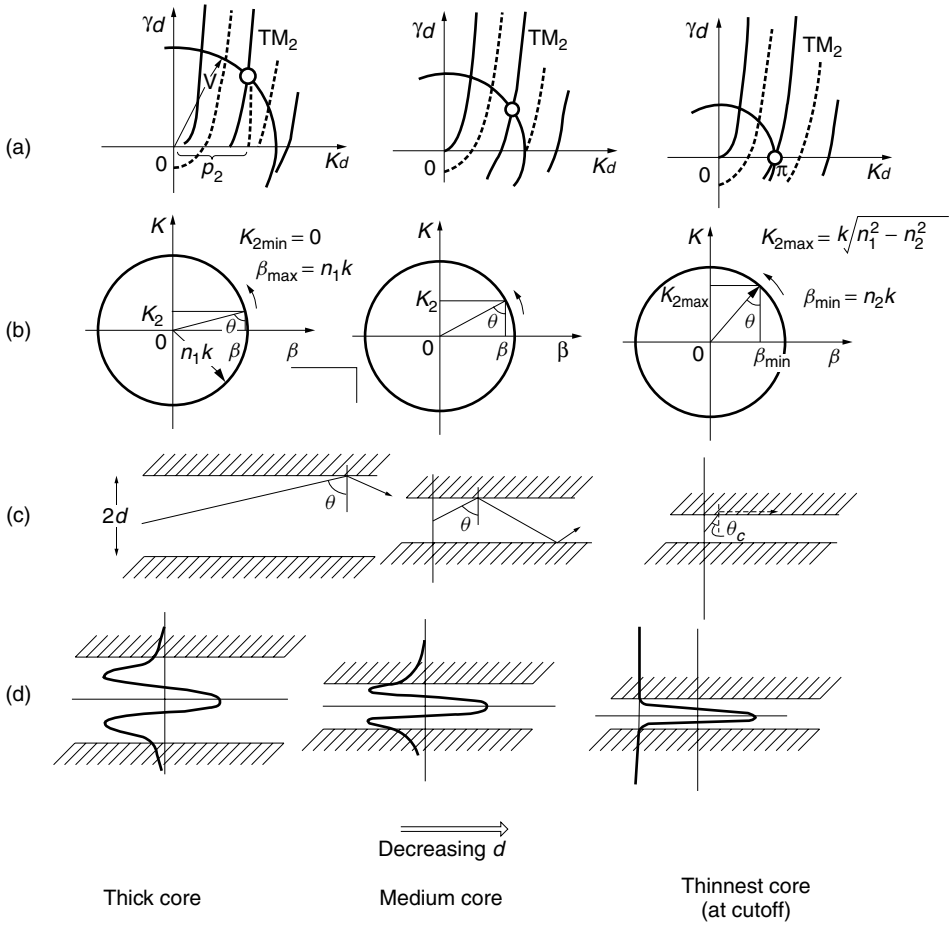

Figure 9.6 Changes to the parameters of the TM_2 mode in a slab optical guide with respect to its core thickness. The left column is the thick core and the right column is the thinnest (at cutoff) core. The free-space wavelength is kept fixed. (a) K–γ diagram. (b) K–β diagram. (c) Component rays. (d) Field pattern in the guide.

as seen from Fig. 9.6a, the decrease in p_2 is much slower than the decrease in d itself (keep in mind that V and d are linearly related) so that the value of K_2 in fact increases with a decrease in d.

(b) With an increase in K_2, the incident angle $\theta_2 = \cos^{-1}(K_2/n_1k)$ decreases. If the value of θ_2 should fall below the critical angle θ_c, then the TM_2 mode ceases to propagate since it leaves the realm of total internal reflection. This can also be explained using Fig. 9.4. With a decrease in $2d$, the null contour line $\overline{RR'}$ has to come down; hence, the angle θ_2 has to be decreased.

(c) Figure 9.6d shows the changes in the cross-sectional distribution of the field. The sinusoidal wave inside the core slightly contracts in the x direction, whereas the evanescent wave in the cladding expands significantly with a decrease in d. □

9.5 EFFECTIVE INDEX OF REFRACTION

First, the concept of the propagation constant β in $e^{j\beta z}$ is reviewed. The propagation constant β is the rate of advance in phase for unit distance (not for unit time) of advance in z. It means that the shorter the wavelength is, the larger the rate of advance in phase for a given distance, and the larger the value of β is.

In free space, the propagation constant is

$$k = \frac{2\pi}{\lambda}$$

where λ is the wavelength in vacuum. If the free space is now filled with a medium with refractive index n_0, the wavelength will be contracted to λ/n_0 and the rate of advance in phase *per distance* will become larger: namely, the propagation constant β_0 in such a medium is

$$\beta_0 = \frac{2\pi}{\lambda/n_0} = n_0 k \tag{9.42}$$

Conversely, the refractive index of the filling medium is given by

$$n_0 = \frac{\beta_0}{k} \tag{9.43}$$

The index of refraction is the ratio of the propagation constant of the medium to that of the vacuum.

Now consider the optical guide. The propagation constant depends on the direction; for instance, it is K in the x direction and it is β in the z direction. In many instances, it is propagation in the z direction that is of principal interest. In the z direction, the guide may be treated as if it were free space filled with a medium with an index of refraction N, defined as

$$N = \frac{\beta}{k} \tag{9.44}$$

where N is called the *effective index of refraction*. The effective index of refraction can be found from Fig. 9.5:

$$\beta = n_1 k \sin\theta$$

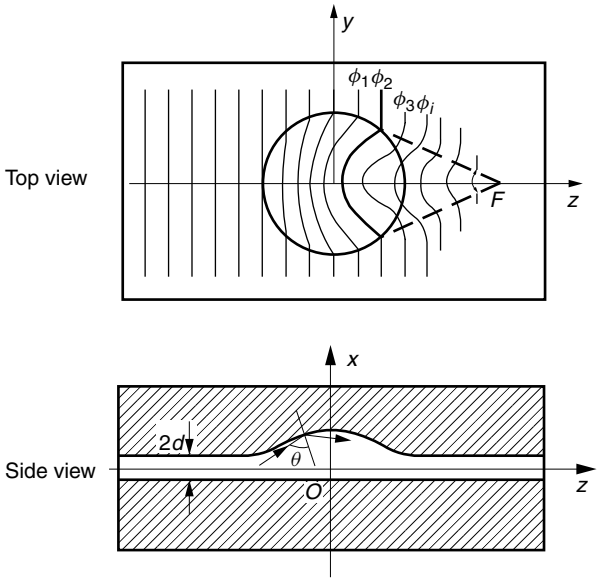

Figure 9.7 Mode-index lens used for integrated optics devices.

and

$$N = n_1 \sin\theta \tag{9.45}$$

Modulation of θ has the same effect as modulating the index of refraction. This effect is used to fabricate integrated optics devices, such as the mode-index lens on a slab guide, shown in Fig. 9.7. When a mode in the guide encounters an increase in guide thickness, the angle θ increases. (This is illustrated in Fig. 9.6b by examining the figure from the right to the left direction, which is the direction of increasing d.) As θ increases, so does the effective refractive index N. For the mode-index lens shown in Fig. 9.7, the advance in constant phase lines is slowed down the most where N is the greatest, and the spacing between the constant phase lines narrows. The result is that the phasefronts of the transmitted wave converge toward the point F.

9.6 TE MODES

The wave optics approach applied earlier to the TM modes is applied in a similar manner to the TE modes. Since the approach is so similar, only the key formulas are repeated for the benefit of summarizing the approach.

The TE modes have only transverse and no longitudinal electric field:

$$E_z = 0 \tag{9.46}$$

Again, the same assumption is made that the guide is excited such that no variation of the field occurs in the y direction, namely,

$$\frac{\partial}{\partial y} = 0 \tag{9.47}$$

With an assumed solution

$$E_y = E_y(x, y)e^{j\beta z - j\omega t} \tag{9.48}$$

the wave equation becomes

$$\frac{1}{E_y}\frac{\partial^2 E_y}{\partial x^2} + [(n_{1,2}k)^2 - \beta^2] = 0 \tag{9.49}$$

The types of solutions of this differential equation depend on the sign of the second term.

If the second term in Eq. (9.49) is a positive constant, the solutions becomes trigonometric functions; whereas if it is a negative constant, the solutions become hyperbolic or exponential functions. In order to suit the physical conditions, the former solutions are used inside the core and the latter inside the cladding:

$$\begin{aligned} (n_1k)^2 - \beta^2 &= K^2 \quad \text{in core} \\ (n_1k)^2 - \beta^2 &= -\gamma^2 \quad \text{in cladding} \end{aligned} \tag{9.50}$$

The solutions of Eq. (9.49) with Eq. (9.50) are

$$E_y = \left\{ \begin{matrix} A\cos Kx, & \text{even TE mode} \\ B\sin Kx, & \text{odd TE mode} \end{matrix} \right\} \quad \text{in core} \tag{9.51}$$

$$E_y = \left\{ \begin{matrix} Ce^{-\gamma x}, & \text{upper layer} \\ De^{\gamma x}, & \text{lower layer} \end{matrix} \right\} \quad \text{in cladding} \tag{9.52}$$

The same notations A, B, C, and D that are used for the TM modes are used for the TE modes, but there is no connection. A factor of $e^{j\beta z - j\omega t}$ is suppressed.

Maxwell's equation $\nabla \times \mathbf{E} = -\partial \mathbf{B}/\partial t$ is used to find H_z:

$$H_z = \frac{1}{j\omega\mu_{1,2}}\frac{\partial E_y}{\partial x} \tag{9.53}$$

where $\mu_{1,2}$ represents the magnetic permeability of the core and cladding layers. Applying Eqs. (9.51) and (9.52) to Eq. (9.53) gives

$$H_z = \frac{K}{j\omega\mu_1}\left\{ \begin{matrix} -A\sin Kx, & \text{even TE mode} \\ B\cos Kx, & \text{odd TE mode} \end{matrix} \right\} \quad \text{in core} \tag{9.54}$$

$$H_z = \frac{\gamma}{j\omega\mu_2}\left\{ \begin{matrix} -Ce^{-\gamma x}, & \text{upper layer} \\ De^{\gamma x}, & \text{lower layer} \end{matrix} \right\} \quad \text{in cladding} \tag{9.55}$$

The other components of the TE modes [5] are

$$\begin{aligned} H_x &= -\frac{\beta}{\omega\mu}E_y \\ E_x &= H_y = E_z = 0 \end{aligned} \tag{9.56}$$

Now, the characteristic equations will be found using the boundary conditions. First, the characteristic equation of the even modes is obtained. From the continuity of E_y at $x = d$,

$$A \cos Kd = Ce^{-\gamma d} \tag{9.57}$$

and from the continuity of H_z at the same boundary,

$$-\frac{K}{j\omega\mu_1} A \sin Kd = -\frac{\gamma}{j\omega\mu_2} Ce^{-\gamma d} \tag{9.58}$$

The division of the above two equations finally gives the characteristic equation for the even TE modes.

$$\left(\frac{\mu_2}{\mu_1}\right) Kd \tan Kd = \gamma d \tag{9.59}$$

Similarly, the continuity of the odd modes gives the characteristic equation for the odd TE modes.

$$-\left(\frac{\mu_2}{\mu_1}\right) Kd \cot Kd = \gamma d \tag{9.60}$$

The difference between the characteristic equations for the TE modes and those for the TM modes is in the factor. The factor for the TE modes is μ_2/μ_1, while that for the TM modes is $(n_2/n_1)^2$. Unless magnetic material is used, $\mu_2/\mu_1 = 1$ and, for the TE modes, the characteristic equations are

$$\begin{aligned} Kd \tan Kd &= \gamma d, \quad \text{even TE mode} \\ -Kd \cot Kd &= \gamma d, \quad \text{odd TE mode} \end{aligned} \tag{9.61}$$

Since the factor $(n_2/n_1)^2$ for the TM modes is close to unity but slightly smaller than unity, the curves of the characteristic equations of the TE modes are almost identical with those of the TM modes shown in Fig. 9.2, but the curves for the TE modes are slightly higher than those of the corresponding TM modes.

9.7 OTHER METHODS FOR OBTAINING THE CHARACTERISTIC EQUATIONS

In Section 9.3, the characteristic equation was derived by the method of wave optics. In this section, a few other available methods are presented. Since the methods will be explained using the simplest geometry, there is little basis for preferring one method over the other; but for more complicated multilayer guides, the choice of the method makes a marked difference in complexity of the treatment. For the sake of comparison, the same geometry and the familiar TM wave are used for all cases.

The three methods described in this section for obtaining the characteristic equation are (1) the coefficient matrix method, (2) the transmission matrix method, and (3) the modified ray model method.

9.7.1 Coefficient Matrix Method

This method is straightforward, but the coefficient matrix is not well suited to multilayer problems because the size of the matrix becomes too cumbersome to manipulate.

The geometry shown Fig. 9.1 is used. The solution for H_y inside the core was given by Eq. (9.9), and that inside the cladding was given by Eq. (9.10). As the first step, terms such as $De^{\gamma x}$ in the upper cladding, which are obviously unfit for physical reasons, are removed. The unfit terms would eventually have been removed automatically by the method, but early removal shortens the procedure.

The constants A, B, C, and D are to be determined using the boundary conditions of continuity of the tangential components of both $\mathbf{E}$ and $\mathbf{H}$ at $x = d$ and $x = -d$. The general solution for H_y in the three layers of a symmetric guide is summarized as

$$\begin{array}{ll} & H_{y2} = Ce^{-\gamma x} \\ x = d: & \hline \\ & H_{y1} = A\cos Kx + B\sin Kx \\ x = -d: & \hline \\ & H_{y3} = De^{\gamma x} \end{array}$$

The tangential $\mathbf{H}$ field is continuous at $x = d$, giving

$$A\cos Kd + B\sin Kd = Ce^{-\gamma d} \tag{9.62}$$

and similarly at $x = -d$,

$$A\cos Kd - B\sin Kd = De^{-\gamma d} \tag{9.63}$$

Since there are four unknown constants, two more independent equations are needed to find a solution. Continuity of the tangential components of the $\mathbf{E}$ field is used. With the help of Eq. (9.21), the E_z fields in the three regions are

$$\begin{array}{ll} & E_{z2} = \dfrac{-jC\gamma}{\omega\epsilon_0\epsilon_{r2}}e^{-\gamma x} \\ x = d: & \hline \\ & E_{z1} = \dfrac{jK}{\omega\epsilon_0\epsilon_r 1}(-A\sin Kx + B\cos Kx) \\ x = -d: & \hline \\ & E_{z3} = \dfrac{jD\gamma}{\omega\epsilon_0\epsilon_{r2}}e^{\gamma x} \end{array}$$

In the top and bottom layers, the relative dielectric constants are ϵ_{r2}, whereas in the core the dielectric constant is ϵ_{r1}. The continuity of the tangential components of the $\mathbf{E}$ field at $x = d$ means that

$$\frac{K}{\epsilon_{r1}}(-A\sin Kd + B\cos Kd) = \frac{-C}{\epsilon_{r2}}\gamma e^{-\gamma d} \tag{9.64}$$

The equation analogous to Eq. (9.64) at the lower $x = -d$ boundary is

$$\frac{K}{\epsilon_{r1}}(A \sin Kd + B \cos Kd) = \frac{D}{\epsilon_{r2}} \gamma e^{-\gamma d} \tag{9.65}$$

Equations (9.62) to (9.65) can be put into matrix form as

$$\begin{matrix} H_y(x=d) \\ H_y(x=-d) \\ E_z(x=d) \\ E_z(x=-d) \end{matrix} \begin{bmatrix} \cos Kd & \sin Kd & -e^{-\gamma d} & 0 \\ \cos Kd & -\sin Kd & 0 & -e^{-\gamma d} \\ -K' \sin Kd & K' \cos Kd & \gamma' e^{-\gamma d} & 0 \\ K' \sin Kd & K' \cos Kd & 0 & -\gamma' e^{-\gamma d} \end{bmatrix} \begin{bmatrix} A \\ B \\ C \\ D \end{bmatrix} = 0 \tag{9.66}$$

where

$$K' = K\frac{1}{\epsilon_{r1}} = \frac{K}{n_1^2}, \quad \gamma' = \gamma\frac{1}{\epsilon_{r2}} = \frac{\gamma}{n_2^2} \tag{9.67}$$

Since the right-hand side of the equation is zero, the determinant has to be zero if a nonzero solution for A, B, C, and D is to exist. The determinant is the characteristic equation. Factoring Eq. (9.66) gives

$$\Delta = e^{-2\gamma d} \cos Kd \sin Kd \begin{vmatrix} 1 & 1 & -1 & 0 \\ 1 & -1 & 0 & -1 \\ -K' \tan Kd & K' \cot Kd & \gamma' & 0 \\ K' \tan Kd & K' \cot Kd & 0 & -\gamma' \end{vmatrix} \tag{9.68}$$

Multiplying the second row by γ', and then subtracting the fourth row from the second row leads to a matrix with the fourth column all zero except at the bottom. The determinant reduces to

$$\Delta = -\tfrac{1}{2} e^{-2\gamma d} \sin 2Kd \begin{vmatrix} 1 & 1 & -1 \\ \gamma' - K' \tan Kd & -\gamma' - K' \cot Kd & 0 \\ -K' \tan Kd & K' \cot Kd & \gamma' \end{vmatrix} \tag{9.69}$$

By multiplying the first row by γ' and then adding the third row to the first row, the determinant reduces to a 2×2 matrix and the characteristic equation finally becomes

$$\Delta = e^{-2\gamma d} \sin 2Kd(\gamma' - K' \tan Kd)(\gamma' + K' \cot Kd) = 0 \tag{9.70}$$

From Eq. (9.70), the determinant is zero when

$$2Kd = n\pi \tag{9.71}$$

or

$$\gamma d = \left(\frac{n_2}{n_1}\right)^2 Kd \tan Kd \tag{9.72}$$

or

$$\gamma d = -\left(\frac{n_2}{n_1}\right)^2 Kd \cot Kd \tag{9.73}$$

Thus, the same results as those in Section 9.3 are obtained. The values of Kd given by Eq. (9.71) are on the cutoff points of the TM modes.

9.7.2 Transmission Matrix Method (General Guides)

This method is especially suited for treating multilayer guides [6,7], such as shown in Fig. 9.8, because, regardless of the number of layers in the guide, the matrices dealt with are always 2×2 matrices. The guide is treated layer by layer, and in each layer the field is expressed by a 2×2 matrix. Using the TM case as an example, the 2×2 matrix gives the relationship between the field $[H_y(x'), E_z(x')]$ at $x = x'$ and the field $[H_y(x), E_z(x)]$ at $x = x$ in that same layer. Using the condition of the continuity of the tangential fields at the boundaries, the fields are connected between the layers.

Let us start with the general solutions of the TM wave, which have been obtained earlier. From Eqs. (9.9) and (9.21), the fields in the ith layer are

$$H_y(x) = A \cos K_i x + B \sin K_i x \tag{9.74}$$

$$E_z(x) = -AZ_i \sin K_i x + BZ_i \cos K_i x \tag{9.75}$$

where

$$Z_i = \frac{jK_i}{\omega \epsilon_0 \epsilon_{ri}} \tag{9.76}$$

or

$$\begin{aligned} Z_i &= \frac{jK_i}{\omega \epsilon_0 n_i^2} \\ K_i &= \sqrt{(n_i k)^2 - \beta^2} \end{aligned} \tag{9.77}$$

We want to choose the values of A and B such that the **H** and **E** fields become the given values of $H(x')$ and $E(x')$ at $x = x'$:

$$H_y(x') = A \cos K_i x' + B \sin K_i x' \tag{9.78}$$

$$E_z(x') = -AZ_i \sin K_i x' + BZ_i \cos K_i x' \tag{9.79}$$

Both x and x' belong to the same ith layer as indicated in Fig. 9.8.

$$x_{i-1} \leq (x', x) \leq x_i$$

where x_{i-1} is the value of x at the lower boundary of the ith layer and x_i is the value of x at the upper boundary of the ith layer. The values of A and B are obtained by

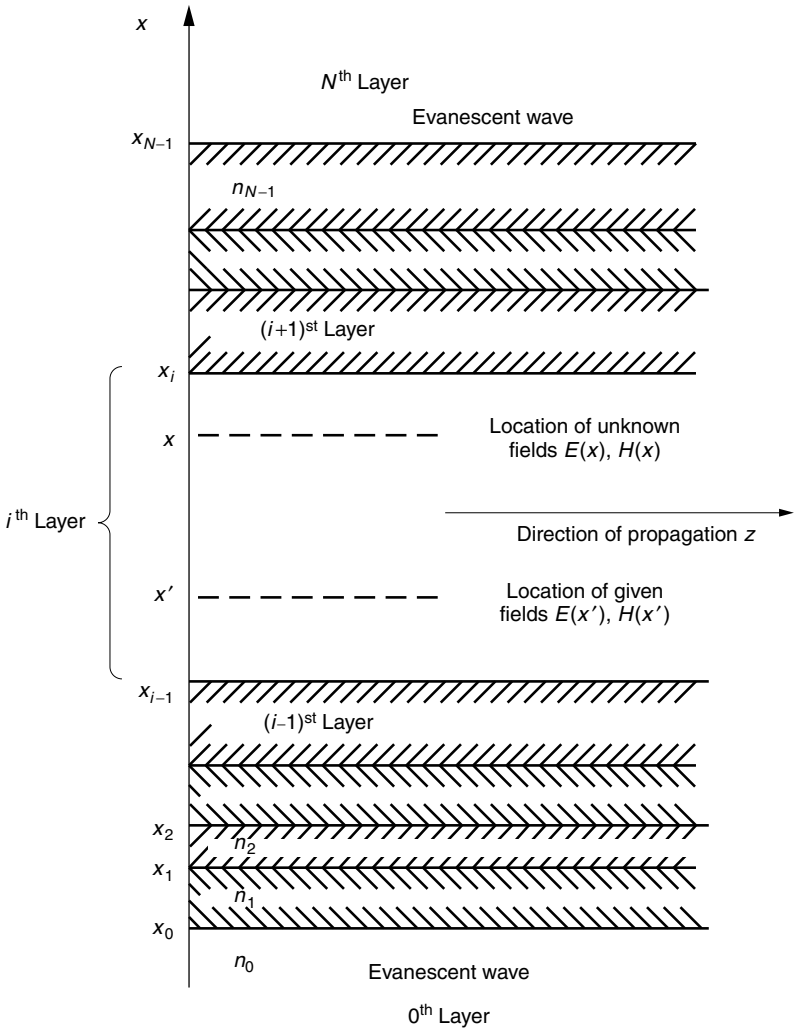

Figure 9.8 Geometry of a layered medium.

solving the simultaneous Eqs. (9.78) and (9.79). The solutions for A and B are put back into Eqs. (9.74) and (9.75) to reach

$$\begin{bmatrix} H_y(x) \\ E_z(x) \end{bmatrix} = \begin{bmatrix} \cos K_i(x-x') & \dfrac{1}{Z_i}\sin K_i(x-x') \\ -Z_i \sin K_i(x-x') & \cos K_i(x-x') \end{bmatrix} \begin{bmatrix} H_y(x') \\ E_z(x') \end{bmatrix} \tag{9.80}$$

Equation (9.80) is the transmission matrix that relates the fields at $x = x'$ with those at $x = x$. The x' and x can be set at any point as long as they belong to the same layer. Equation (9.80) is the only type of matrix that is needed for the transmission matrix method.

The transmission matrix method will first be illustrated using the example of a three-layer guide with the geometry shown in Fig. 9.9. The core-cladding lower boundary

was placed at $x = 0$ and the upper boundary at $x = 2d$. All other parameters are the same as before. Only one transmission matrix is needed for this geometry:

$$\begin{bmatrix} H_y(2d) \\ E_z(2d) \end{bmatrix} = \begin{bmatrix} \cos 2Kd & \dfrac{1}{Z_1}\sin 2Kd \\ -Z_1 \sin 2Kd & \cos 2Kd \end{bmatrix} \begin{bmatrix} H_y(0) \\ E_z(0) \end{bmatrix} \tag{9.81}$$

The geometry of the layers alone can never determine the field inside the medium. It is only after the fields on the boundary are specified that the field inside the medium is determined. The specification of the field can be the field H_y or E_z itself, as in the case of a given incident field to the boundary; or the field specification can be an unbounded traveling wave, a ratio of reflected to incident waves (standing wave), or an evanescent wave. These are called boundary fields. This section deals with guides whose boundary fields are evanescent waves.

Now let us deal with the case of a guide for which the fields in the bottom layer as well as in the top layer are unbounded waves. The unbounded field in the bottom layer is the evanescent wave $H_{y0}(x)$, which is expressed by the bottom equation of Eq. (9.11). The bottom equation of Eq. (9.11) is inserted into Eq. (9.21) to obtain

$$E_{z0}(x) = \frac{j}{\omega\epsilon_r\epsilon_0}\frac{\partial}{\partial x}De^{\gamma_0 x} = Z_0 H_{y0}(x) \tag{9.82}$$

where

$$Z_0 = \frac{j\gamma_0}{\omega\epsilon_0 n_0^2} \tag{9.83}$$

The unbounded field $H_{y2}(x)$ in the top layer is also an evanescent wave and is expressed by the top equation of Eq. (9.11). Inserting the top equation of Eq. (9.11) into Eq. (9.21) gives

$$E_{z2}(x) = \frac{j}{\omega\epsilon_0\epsilon_2}\frac{\partial}{\partial x}Ce^{-\gamma_2 x} = -Z_2 H_{y2}(x) \tag{9.84}$$

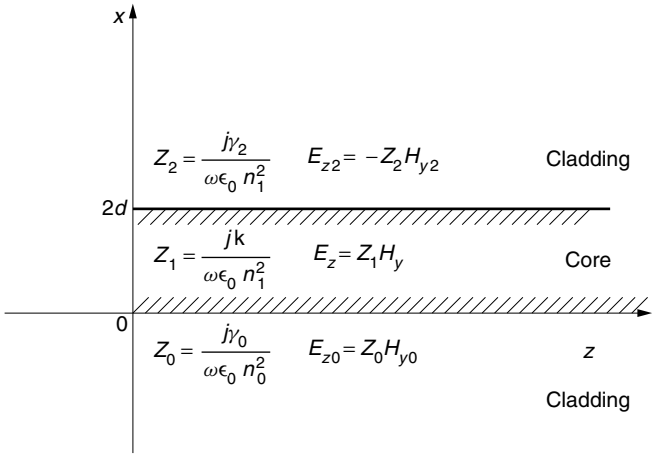

Figure 9.9 Geometry of the three-layer slab guide.

where

$$Z_2 = \frac{j\gamma_2}{\omega\epsilon_0 n_2^2} \tag{9.85}$$

The minus sign on the right-hand side of Eq. (9.84) should be noted. For simplicity, the second subscripts will be dropped as

$$\begin{aligned} H_{y0}(0) &= H_y(0) \qquad E_{z0}(0) = E_z(0) \\ H_{y2}(2d) &= H_y(2d) \quad E_{z2}(2d) = E_z(2d) \end{aligned} \tag{9.86}$$

The $E_z(2d)$ and $E_z(0)$ in Eq. (9.81) are rewritten in terms of $H_y(2d)$ and $H_y(0)$, applying the boundary conditions to Eqs. (9.82) and (9.84) and rearranged as

$$\begin{bmatrix} \cos 2Kd + \dfrac{Z_0}{Z_1}\sin 2Kd & -1 \\ Z_0 \cos 2Kd - Z_1 \sin 2Kd & Z_2 \end{bmatrix} \begin{bmatrix} H_y(0) \\ H_y(2d) \end{bmatrix} = 0 \tag{9.87}$$

In order that $H_y(0)$ and $H_y(2d)$ have nonzero solutions, the determinant has to be zero. The determinant is

$$(Z_0 + Z_2)\cos 2Kd - \left(Z_1 - \frac{Z_0 Z_2}{Z_1}\right)\sin 2Kd = 0 \tag{9.88}$$

or

$$\frac{Z_0/Z_1 + Z_2/Z_1}{1 - Z_0 Z_2/Z_1^2} = \tan 2Kd \tag{9.89}$$

If the guide is symmetric and $Z_2 = Z_0$, then

$$\frac{2(Z_0/Z_1)}{1 - (Z_0/Z_1)^2} = \tan 2Kd \tag{9.90}$$

The trigonometric identity

$$\tan 2Kd = \frac{2\tan Kd}{1 - \tan^2 Kd}$$

is inserted into Eq. (9.90). After rearrangement, Eq. (9.90) becomes

$$\left(\frac{\gamma}{n^2 K} - \tan Kd\right)\left(\frac{\gamma}{n^2 K}\tan Kd + 1\right) = 0 \tag{9.91}$$

where Eqs. (9.76) and (9.83) were used to rewrite

$$Z_0/Z_1 = \frac{\gamma}{n^2 K}$$

Thus, the first factor of Eq. (9.91) is the characteristic equation for the even TM modes and the second, for the odd TM modes.

Next, this method will be extended to an $(N-1)$-layer guide in unbounded space. The continuity condition is used to connect the field of one layer to the next. As already

stated, in the two outermost layers, the wave is necessarily an evanescent wave, and the first and last layers are set aside for now. The matrix that applies to the ith layer in the geometry shown in Fig. 9.8 is, from Eq. (9.80),

$$\begin{bmatrix} H_y(x_i) \\ E_z(x_i) \end{bmatrix} = [T_i(x_i - x_{i-1})] \begin{bmatrix} H_y(x_{i-1}) \\ E_z(x_{i-1}) \end{bmatrix} \tag{9.92}$$

where

$$T_i(x_i - x_{i-1}) = \begin{bmatrix} \cos K_i(x_i - x_{i-1}) & \dfrac{1}{Z_i} \sin K_i(x_i - x_{i-1}) \\ -Z_i \sin K_i(x_i - x_{i-1}) & \cos K_i(x_i - x_{i-1}) \end{bmatrix} \tag{9.93}$$

In the event that a particular mode that has an evanescent wave in the ith layer is desired, the transmission matrix $T_i(x_i - x_{i-1})$ of the ith layer has to be derived in a similar manner as Eq. (9.93) was derived from Eqs. (9.74) and (9.75), starting from

$$H_y(x) = C \cosh \gamma_i x + D \sinh \gamma_i x \tag{9.94}$$

$$E_z(x) = Z_i C \sinh \gamma_i x + Z_i D \cosh \gamma_i x \tag{9.95}$$

where

$$\gamma_i = \sqrt{\beta^2 - (n_i k)^2} \tag{9.96}$$

$$Z_i = \frac{j\gamma_i}{\omega \epsilon_0 \epsilon_{ri}} \tag{9.97}$$

The values of C and D are chosen such that H and E become $H(x')$ and $E(x')$ at $x = x'$. These values of C and D are put back into Eqs. (9.94) and (9.95). The obtained matrix is

$$T_i^e(x_i - x_{i-1}) = \begin{bmatrix} \cosh \gamma_i(x_i - x_{i-1}) & \dfrac{1}{Z_i} \sinh \gamma_i(x_i - x_{i-1}) \\ Z_i \sinh \gamma_i(x_i - x_{i-1}) & \cosh \gamma_i(x_i - x_{i-1}) \end{bmatrix} \tag{9.98}$$

Compared to Eq. (9.93), the lower left element has a positive sign instead of a negative sign, and the sine and cosine functions are changed to hyperbolic functions.

Repeated use of Eq. (9.92) to connect the field starting from the first layer up the $(N-1)$st layer gives $[T_{N-1}][T_{N-2}] \cdots [T_1]$:

$$\begin{bmatrix} H_y(x_{N-1}) \\ E_z(x_{N-1}) \end{bmatrix} = [T_{N-1}][T_{n-2}] \cdots [T_i] \cdots [T_1] \begin{bmatrix} H_y(x_0) \\ E_z(x_0) \end{bmatrix} \tag{9.99}$$

The product of the T matrices is rewritten as

$$\begin{bmatrix} H_y(x_{N-1}) \\ E_z(x_{N-1}) \end{bmatrix} = \begin{bmatrix} A & B \\ C & D \end{bmatrix} \begin{bmatrix} H_y(x_0) \\ E_z(x_0) \end{bmatrix} \tag{9.100}$$

Now, the field at the top boundary of the zeroth layer is

$$E_z(x_0) = Z_0 H_y(x_0) \tag{9.101}$$

where

$$Z_0 = \frac{j\gamma_0}{\omega \epsilon_0 n_0^2} \tag{9.102}$$

and

$$\gamma_0 = \sqrt{\beta^2 - (n_0 k)^2} \tag{9.103}$$

The field at the lower boundary of the top free-space layer, which is the top boundary of the $(N-1)$st layer has a similar relationship as Eq. (9.84) and

$$E_z(x_{N-1}) = -Z_N H_y(x_{N-1}) \tag{9.104}$$

where

$$Z_N = \frac{j\gamma_N}{\omega\epsilon_0 n_N^2} \tag{9.105}$$

and

$$\gamma_N = \sqrt{\beta^2 - (n_N k)^2} \tag{9.106}$$

Note the difference in signs in Eqs. (9.101) and (9.104). Also note that the Nth layer is free space and Z_N given by Eq. (9.104) has to be used.

It may be added that, as explained in Section 2.7.1, the z-direction propagation constant β in the zeroth layer given by Eq. (9.103) is the same as that in the Nth layer given by Eq. (9.106) because the fields in both layers satisfy Eq. (9.1).

As a matter of fact, the fields in every layer satisfy Eq. (9.1) and have the same value of β. The phase match condition in the z direction is automatically satisfied across every layer boundary. The expressions for $E_z(x_{N-1})$ and $E_z(x_0)$ are rewritten in terms of $H_y(x_{N-1})$ and $H_y(x_0)$ using Eqs. (9.101) and (9.104) and are incorporated into Eq. (9.100):

$$\begin{bmatrix} A + Z_0 B & -1 \\ C + Z_0 D & Z_N \end{bmatrix} \begin{bmatrix} H_y(x_0) \\ H_y(x_{N-1}) \end{bmatrix} = 0 \tag{9.107}$$

In order that the solutions for $H_y(x_0)$ and $H(x_{N-1})$ are nonzero, the determinant of Eq. (9.107) has to be zero. Thus, the characteristic equation is finally

$$Z_N A + Z_0 Z_N B + C + Z_0 D = 0 \tag{9.108}$$

where the values of Z_0 and Z_N are available from Eqs. (9.102) and (9.105) and the matrix elements A, B, C, and D are obtained after calculating the product of the T's in Eq. (9.99). See the example of the asymmetric three-layer case in Example 9.6.

9.7.3 Transmission Matrix Method (Symmetric Guide)

If symmetry exists in the distribution of the indices of refraction, the computation becomes significantly simpler. Let us say, as shown in Fig. 9.10, symmetry exists with respect to $x = 0$ and the indices of refraction from the bottom to the top layer are arranged as $n_0, n_1, n_2, \ldots, n_{n-1}, n_{n-1}, \ldots, n_2, n_1, n_0$. The transmission matrix then becomes

$$[T_1][T_2]\cdots[T_{n-1}]\cdot[T_{n-1}]\cdots[T_2][T_1] \tag{9.109}$$

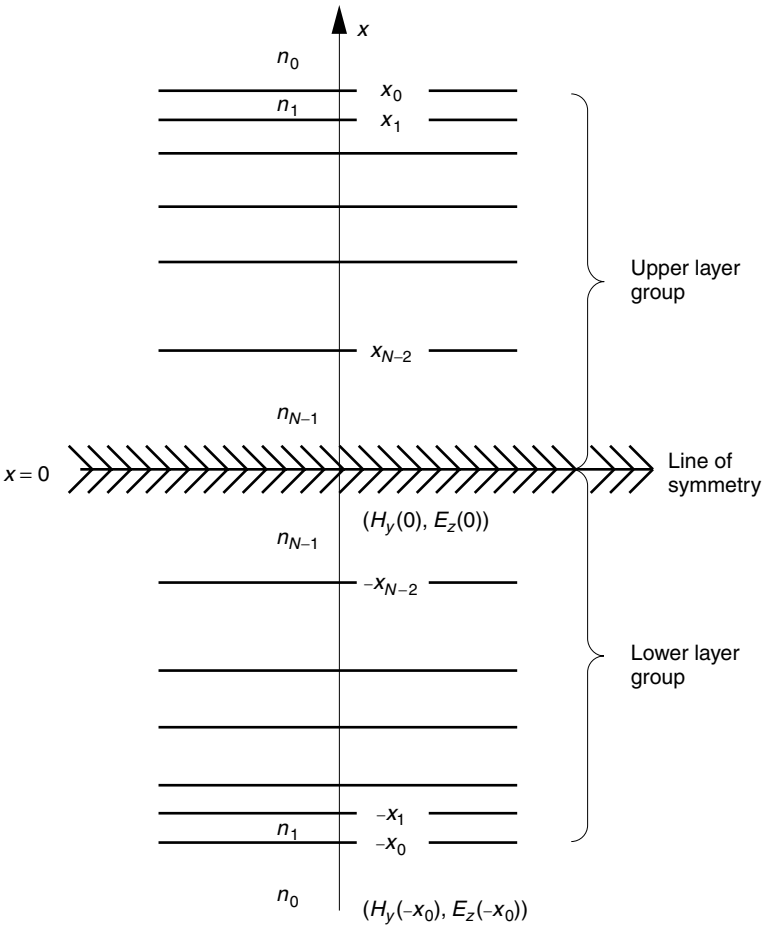

Figure 9.10 Geometry of layers with symmetry with respect to $x = 0$.

where the zeroth layer is considered unbounded and will be treated separately, as was done in Eq. (9.101). Equation (9.109) is now divided into two layer groups:

$$T_+ = [T_1][T_2]\cdots[T_{n-1}] \tag{9.110}$$

$$T_- = [T_{n-1}]\cdots[T_2][T_1] \tag{9.111}$$

Noting that with either Eq. (9.93) or (9.98) if

$$[T_1][T_2] = \begin{bmatrix} a & b \\ c & d \end{bmatrix}$$

then

$$[T_2][T_1] = \begin{bmatrix} d & b \\ c & a \end{bmatrix}$$

because in both formulas the two diagonal elements in $[T_i]$ are identical.

Let

$$T_- = \begin{bmatrix} A & B \\ C & D \end{bmatrix} \tag{9.112}$$

then T_+, which consists of the same matrices but in reverse order in multiplication, becomes

$$T_+ = \begin{bmatrix} D & B \\ C & A \end{bmatrix} \tag{9.113}$$

Thus, the characteristic matrix

$$[T] = [T_+][T_-] \tag{9.114}$$

is obtained by the product of Eqs. (9.112) and (9.113) as

$$[T] = \begin{bmatrix} AD + BC & 2BD \\ 2AC & AD + BC \end{bmatrix} \tag{9.115}$$

The $[T]$ can be obtained by first calculating A, B, C, and D of T_- and then using them in Eq. (9.115). The characteristic matrix thus obtained involves only about one-half of the number of matrix multiplications.

The calculation of the modes in the symmetric structure can be simplified further by calculating the even and odd modes separately. Even and odd refers to H_y for the TM modes.

A special feature of the even modes is that not only is the field distribution in the upper layer group symmetric with that in the lower layer group with respect to $x = 0$, but also the derivative dH_y/dx has to vanish at $x = 0$ for a smooth connection.

$$\left.\frac{dH_y}{dx}\right|_{x=0} = 0 \quad \text{means} \quad E_z(0) = \left.\frac{j}{\omega\epsilon_0\epsilon_r}\frac{dH_y}{dx}\right|_{x=0} = 0 \tag{9.116}$$

As mentioned earlier, at the lowest boundary

$$E(-x_0) = Z_0 H_y(-x_0)$$

The field in the lower layer group is, from Eqs. (9.100) and (9.116),

$$\begin{bmatrix} H_y(0) \\ 0 \end{bmatrix} = \begin{bmatrix} A & B \\ C & D \end{bmatrix} \begin{bmatrix} H_y(-x_0) \\ Z_0 H_y(-x_0) \end{bmatrix} \tag{9.117}$$

Equation (9.117) can be rewritten as

$$\begin{bmatrix} A + Z_0 B & -1 \\ C + Z_0 D & 0 \end{bmatrix} \begin{bmatrix} H_y(-x_0) \\ H_y(0) \end{bmatrix} = 0 \tag{9.118}$$

For $H_y(-x_0)$ and $H_y(0)$ to exist, the determinant has to vanish and the characteristic equation for the even modes is given by

$$C + Z_0 D = 0 \tag{9.119}$$

Next, the characteristic equation for the odd TM modes is derived. A special feature of the odd modes is that not only is the field in the upper layer group the negative of the corresponding field in the lower layer group, but also the field itself has to vanish at $x = 0$ and $H_y(0) = 0$ so as to connect at $x = 0$.

$$\begin{bmatrix} 0 \\ E_z(0) \end{bmatrix} = \begin{bmatrix} A & B \\ C & D \end{bmatrix} \begin{bmatrix} H_y(-x_0) \\ Z_0 H_y(-x_0) \end{bmatrix} \tag{9.120}$$

Equation (9.120) can be rewritten as

$$\begin{bmatrix} A + Z_0 B & 0 \\ C + Z_0 D & -1 \end{bmatrix} \begin{bmatrix} H(-x_0) \\ E_z(0) \end{bmatrix} = 0 \tag{9.121}$$

For $H(-x_0)$ and $E_z(0)$ to exist, the determinant has to vanish and the characteristic equation for the odd modes is given by

$$A + Z_0 B = 0 \tag{9.122}$$

Example 9.5 Derive the characteristic equation of a planar type W guide (named after the shape of the index of refraction). The geometry and the indices of refraction are shown in Fig. 9.11.

Solution Calculation will take an advantage of the symmetry in the guide structure. Since $n_1 > n_2$, the guided waves can be in the center region. No total internal reflection exists at $x = \pm(d_1 + d_2)$ and this boundary alone cannot be used for confinement. The guided wave exists in $d_1 > x > -d_1$ only when the waves in $d_1 < |x| < d_1 + d_2$ are evanescent waves.

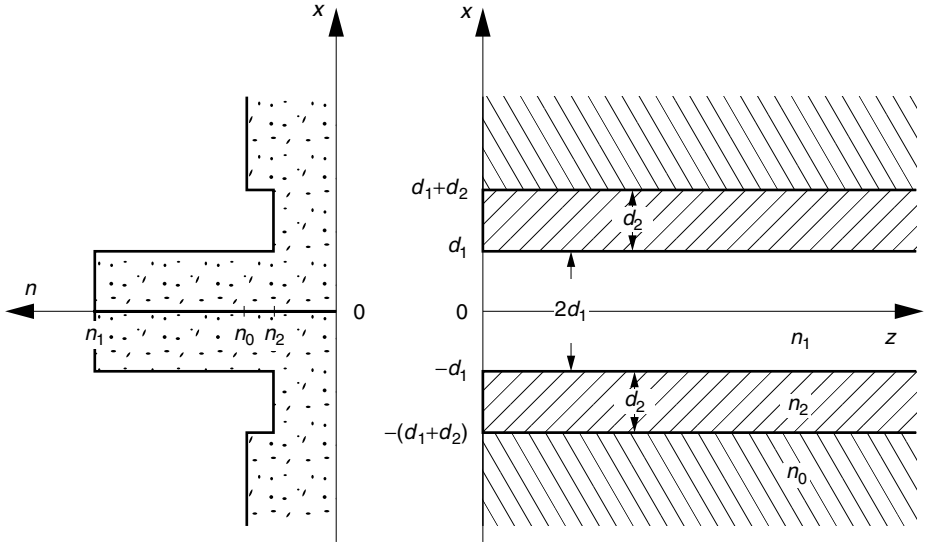

Figure 9.11 Geometry of the planar W guide.

In the region $-(d_1 + d_2) < x < -d_1$, from Eqs. (9.97) and (9.98), T_1 is

$$T_1 = \begin{bmatrix} \cosh \gamma_2 d_2 & \dfrac{1}{Z_2} \sinh \gamma_2 d_2 \\ Z_2 \sinh \gamma_2 d_2 & \cosh \gamma_2 d_2 \end{bmatrix} \tag{9.123}$$

with

$$Z_2 = \frac{j\gamma_2}{\omega \epsilon_0 n_2^2} \tag{9.124}$$

In the region $-d_1 < x < 0$, from Eqs. (9.76) and (9.93), T_2 is

$$T_2 = \begin{bmatrix} \cos K_1 d_1 & \dfrac{1}{Z_1} \sin K_1 d_1 \\ -Z_1 \sin K_1 d_1 & \cos K_1 d_1 \end{bmatrix} \tag{9.125}$$

with

$$Z_1 = \frac{jK_1}{\omega \epsilon_0 n_1^2} \tag{9.126}$$

Next, from T_2 and T_1, the matrix $T_- = [T_2][T_1]$ is calculated and then the matrix elements in T_- are used to find the characteristic equations by Eqs. (9.119) and (9.122).

For the even modes

$$\begin{aligned} &- Z_1 \tan K_1 d_1 + Z_2 \tanh \gamma_2 d_2 \\ &+ Z_0 \left(1 - \frac{Z_1}{Z_2} \tan K_1 d_1 \tanh \gamma_2 d_2 \right) = 0 \end{aligned} \tag{9.127}$$

which can be rewritten as

$$Z_0 = Z_1 \left(\frac{1 - A/B}{1 - AB} \right) \tan K_1 d_1 \tag{9.128}$$

where

$$A = \tanh \gamma_2 d_2 \tag{9.129}$$

$$B = \frac{Z_1}{Z_2} \tan K_1 d_1 \tag{9.130}$$

Equation (9.128) can be rewritten using Eqs. (9.102), (9.124), and (9.126). Thus, the characteristic equation for the even TM modes is

$$\gamma_0 d_1 = \left(\frac{n_0}{n_1} \right)^2 K_1 d_1 \left(\frac{1 - A/B}{1 - AB} \right) \tan K_1 d_1 \tag{9.131}$$

$$B = \left(\frac{n_2}{n_1} \right)^2 \frac{K_1}{\gamma_2} \tan K_1 d_1 \tag{9.132}$$

The result can be verified by setting either $d_2 \to 0$ or $n_2 \to n_0$. If $d_2 \to 0$, then $A = 0$ and Eq. (9.131) immediately reduces to Eq. (9.72). If $n_2 \to n_0$ and hence $\gamma_2 \to \gamma_0$, then B in Eq. (9.132) approaches unity because Eq. (9.72) can be approximately used in Eq. (9.132), and Eq. (9.131) approaches Eq. (9.72).

The procedure for calculating β for given physical parameters will be described. From Eqs. (9.77) and (9.96), the attentuation and propagation constants are

$$K_1 = \sqrt{(n_1 k)^2 - \beta^2} \tag{9.133}$$

$$\gamma_0 = \sqrt{\beta^2 - (n_0 k)^2} \tag{9.134}$$

$$\gamma_2 = \sqrt{\beta^2 - (n_2 k)^2} \tag{9.135}$$

From Eqs. (9.133) and (9.134), V_0^2 is expressed as

$$V_0^2 = (K_1 d_1)^2 + (\gamma_0 d_1)^2 \tag{9.136}$$

where

$$V_0 = k d_1 \sqrt{n_1^2 - n_0^2} \tag{9.137}$$

Similarly, from Eqs. (9.133) and (9.135), V_2^2 is expressed as

$$V_2^2 = (K_1 d_1)^2 + (\gamma_2 d_1)^2 \tag{9.138}$$

where

$$V_2 = k d_1 \sqrt{n_1^2 - n_2^2} \tag{9.139}$$

The procedures to find β are as follows:

1. Calculate both V_0 and V_2 from Eqs. (9.137) and (9.139).
2. Use $\gamma_2 d_1 = \sqrt{V_2^2 - (K_1 d_1)^2}$ to calculate $\gamma_2 d_1$ for a given $K_1 d_1$.
3. Insert γ_2 and the given value of $K_1 d_1$ into Eqs. (9.129) and (9.132) to find A and B and hence the corresponding value of $\gamma_0 d_1$ for the given $K_1 d_1$ from Eq. (9.131). Repeat the same with the other values of $K_1 d_1$ to complete such curves as shown in Fig. 9.12.
4. The intersections between the above curves and the circle of Eq. (9.136) are the desired solutions.
5. From Eq. (9.133), β is calculated for the obtained value of K_1.

As shown in Fig. 9.12, the value of $K_1 d_1$ for the W guide is shifted from that of the three-layer symmetric guide shown in Fig. 9.2. One of the determining factors of the distortion of a light pulse during the transmission in the guide is $d\beta^2/d\omega^2$ as will be detailed in Chapter 11. The values of n_2 and d_2 are manipulated to make a distortion-free line out of the W guide.

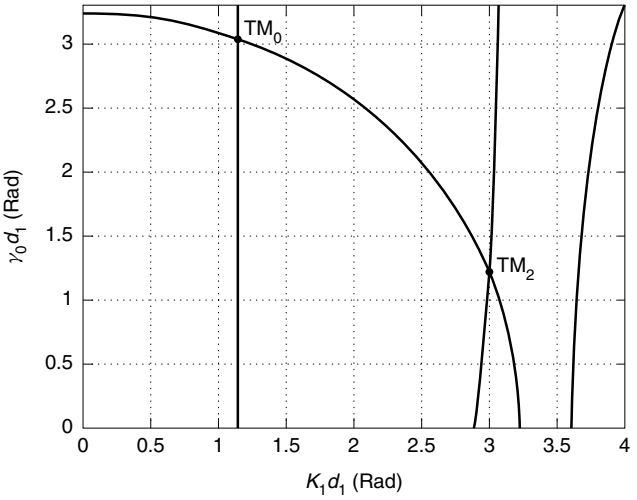

Figure 9.12 Graphical solution of the planar W guide for the even TM modes. The physical parameters are $\lambda = 1.3$ μm, $d_1 = 0.9$ μm, $d_2 = 1.0$ μm, $n_0 = 3.44$, $n_1 = 3.5$, and $n_2 = 3.42$. (Calculation courtesy of H. S. Loka.)

The characteristic equation for the odd TM modes can be obtained in a similar manner and the result is

$$\gamma_0 d_1 = -\left(\frac{n_0}{n_1}\right)^2 K_1 d_1 \cot K_1 d \cdot \left(\frac{1 + AB'}{1 + A/B'}\right) \tag{9.140}$$

where A is given by Eq. (9.129) and

$$B' = \frac{z_2}{z_1} \tan K_1 d_1$$

The result can be verified by setting either $d_2 \to 0$ or $n_2 \to n_0$, as in the case of the even TM modes. □

9.7.4 Modified Ray Model Method

The mode is essentially a quantization of the propagation constant, or a quantization of the angle of propagation of the component plane waves. At angles other than the quantized angles, no light can propagate in the guide. In Section 9.4, it was shown that a mode in the guide could be thought of as the standing-wave pattern of two component waves, one propagating in a slightly downward direction and the other in a slightly upward direction. Figure 9.13 shows the path of the component rays inside the optical guide. The hatched bell-shaped curve signifies the transverse distribution of the light. The field at $x = x_1$ for the downward component wave is considered first. As illustrated in Fig. 9.13, the field at any given point along $x = x_1$ is the sum of numerous contributing fields due to the transverse spread of the beam. If the beam were a plane wave, the transverse spread would be wider, and the interference would be even bigger. If the phases of the contributing fields are random, the resultant travelling wave field becomes null. If, however, the phase shift associated with one round trip is an integral multiple of 2π radians, all the contributing fields interfere constructively, and the field

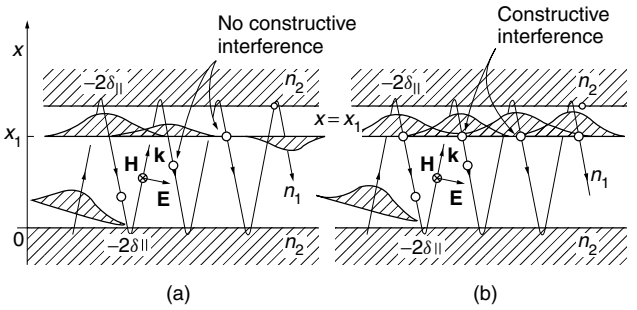

Figure 9.13 Explanation of the quantization in the x direction. (a) Random phase at $x = x_1$. (b) In phase at $x = x_1$. $4Kd - 4\delta_{\|} = 2\,\mu\pi$.

builds up. The phase shift associated with one round trip includes the phase shifts due to the total internal reflections at the top and bottom boundaries as well as the phase shift due to the round-trip distance inside the guide.

The same is true with the upward component wave. The field at any given point is the sum of many contributing fields, which must interfere constructively for the field to build up, and the same condition applies that the round-trip phase shift be an integral multiple of 2π.

The upward and downward component waves propagating in opposite directions again interfere and generate a standing-wave pattern, which is the mode pattern of the guide.

The amount of the phase shift associated with the reflection from the boundary depends on the direction of the polarization of the component plane wave. As shown in Fig. 9.13, if the TM wave is used, the direction of the **H** field is perpendicular to the plane of propagation and, hence, the direction of the polarization of the **E** field is parallel to the plane of propagation (in the plane of the page). The total round-trip phase shift for a $2d$-thick guide for constructive interaction is

$$4Kd - 4\delta_{\|} = 2\mu\pi \tag{9.141}$$

where μ is an integer and the phase shift due to the total internal reflections at each boundary is $-2\delta_{\|}$ as given by Eq. (2.86). Equation (9.141) is sometimes called the *dispersion equation*.

With Eq. (2.91), Eq. (9.141) becomes

$$\tan\left(Kd - \frac{\pi}{2}\mu\right) = \frac{\gamma}{n^2 K} \tag{9.142}$$

where

$$n = \frac{n_2}{n_1}$$

The integer μ is the mode number and separating it into even and odd modes gives

$$\tan Kd = \frac{\gamma}{n^2 K} \quad \text{for even } \mu \tag{9.143}$$

$$-\cot Kd = \frac{\gamma}{n^2 K} \quad \text{for odd } \mu \tag{9.144}$$

Thus, these results are identical to the results with the other three methods.

In the case of multilayer guides, the fields that are reflected from each interface must be taken into account in order to calculate the resultant phase shift, and calculation by this method becomes difficult.

9.8 ASYMMETRIC OPTICAL GUIDE

The three-layer optical guide with a different index of refraction for each layer is investigated in this section. Even though the analysis is slightly more complex, the asymmetric guide is of more practical importance than the symmetric guide. The geometry of the guide under consideration is shown in Fig. 9.14. The thickness of the film (core layer) is $2d$ and its index of refraction is n_1. The index of refraction of the substrate (cladding layer) is n_2. Very often, the top layer is air but sometimes it is a covering medium. The index of refraction of the top layer is n_0.

The characteristic equation for an asymmetric guide is derived by modifying the dispersion equation for the symmetric guide. The phase shift due to total internal reflection in Eq. (9.141) is separated into two parts, and with this modification, Eq. (9.141) becomes

$$4Kd - 2\delta_{\parallel}^{c} - 2\delta_{\parallel}^{s} = 2\mu\pi \tag{9.145}$$

where $-2\delta_{\parallel}^{c}$ is the phase shift due to the reflection at the air–film or cover–film interface and $-2\delta_{\parallel}^{s}$ is that of the film-substrate interface. From Eq. (2.91), the values of $\delta_{\parallel}^{c}$ and $\delta_{\parallel}^{s}$ are known and Eq. (9.145) becomes

$$(2Kd - \mu\pi) = \tan^{-1}\left(\frac{\gamma_0}{n_0'^2 K}\right) + \tan^{-1}\left(\frac{\gamma_2}{n_2'^2 K}\right) \tag{9.146}$$

where

$$n_0' = \frac{n_0}{n_1}, \quad n_2' = \frac{n_2}{n_1}$$

Equation (9.146) can be rewritten by recalling the identities

$$\tan(\theta_1 + \theta_2) = \frac{\tan\theta_1 + \tan\theta_2}{1 - \tan\theta_1 \tan\theta_2} \tag{9.147}$$

$$\tan(\theta - \mu\pi) = \tan\theta \tag{9.148}$$

With the help of these identities, the characteristic equation for the asymmetric guide is

$$\frac{K\left(\dfrac{\gamma_0}{n_0'^2} + \dfrac{\gamma_2}{n_2'^2}\right)}{K^2 - \dfrac{\gamma_0\gamma_2}{n_0'^2 n_2'^2}} = \tan 2Kd \tag{9.149}$$

Equation (9.149) becomes identical with Eq. (9.89) obtained by the transmission matrix method if the relationships Eqs. (9.102), (9.124), and (9.126) are used.

There are three unknowns — K, γ_0, and γ_2 — in Eq. (9.149), and in order to find a solution, more formulas are needed. The propagation constant relationships across a

boundary were discussed in Section 2.7.1. Because of phase matching, the propagation constant β in the z direction is the same for every layer and

$$K = \sqrt{(n_1 k)^2 - \beta^2} \tag{9.150}$$

$$\gamma_0 = \sqrt{\beta^2 - (n_0 k)^2} \tag{9.151}$$

$$\gamma_2 = \sqrt{\beta^2 - (n_2 k)^2} \tag{9.152}$$

Now, there are four unknowns — K, γ_0, γ_2, and β; and there are four equations — Eqs. (9.149) to (9.152). By substituting Eqs. (9.150) through (9.152) into Eq. (9.149), an equation in terms of β is obtained. Unfortunately, this equation is a transcendental equation and no closed-form solutions are possible, but the solutions can be obtained by numerical methods. The solutions for a specific optical guide are shown in the next example.

Example 9.6 An asymmetric optical guide such as the one shown in Fig. 9.14 is fabricated by depositing a glass film with a higher index of refraction over a glass substrate. The film thickness is $2d$. The indices of refraction are $n_0 = 1$, $n_1 = 1.55$, and $n_2 = 1.54$ and the TM modes are excited. The wavelength is λ. The positive x direction is taken downward.

Without any elaborate numerical calculations, make intelligent guesses at the following:

(a) The total number of possible modes.
(b) The conditions for a single mode guide.
(c) The field distributions for the first few mode orders.
(d) The correlation of the region of β with the field pattern and directions of propagation of the component plane waves.

Solution The change in the index of refraction at the air–film interface is much greater than that at the film–substrate interface. Therefore, if the condition of total

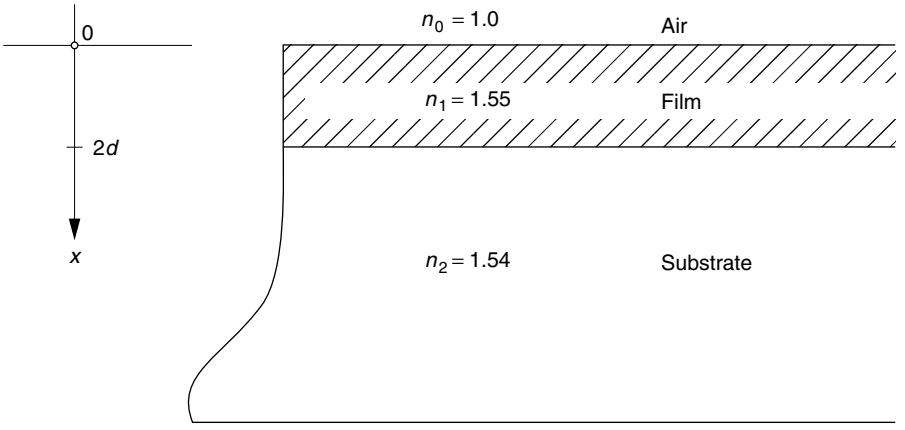

Figure 9.14 Geometry of an asymmetric slab optical guide.

internal reflection for the film–substrate is satisfied, that for the air–film is automatically satisfied. Hence, the results are primarily determined by the film–substrate boundary.

First, the region of β is investigated. Using Eqs. (9.150) to (9.152) and the given physical parameters, the curves for K, γ_0, and γ_1 are plotted as a function of β in Fig. 9.15a. The upper limit of β is determined by the index of refraction of the film $n_1 k$ from Eq. (9.150).

$$n_1 k > \beta \tag{9.153}$$

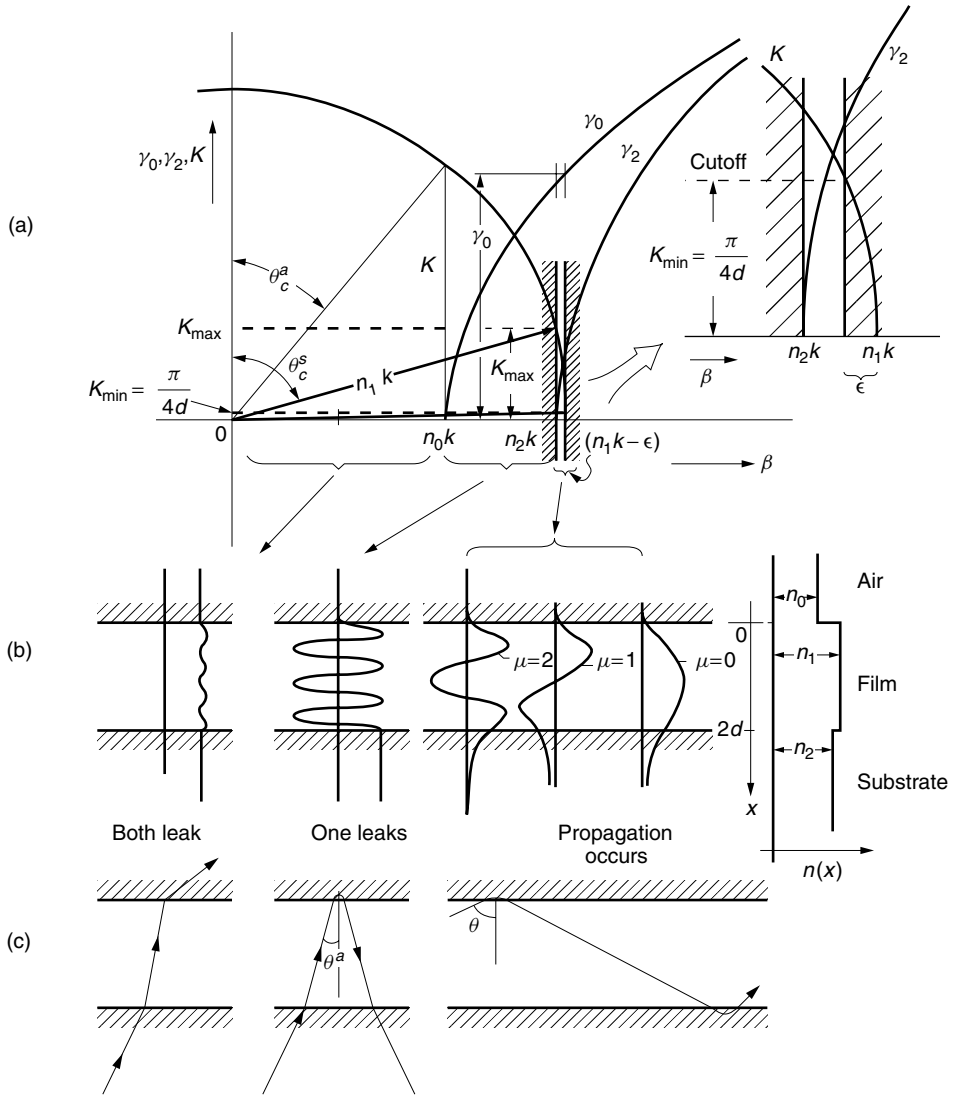

Figure 9.15 Combined chart of an asymmetric optical guide. (a) $K-\beta$ diagram. (b) Amplitude distribution. (c) Ray path.

The lower limit of β is determined by the condition of the cutoffs (total internal reflection) at the air–film and the film–substrate boundaries. From Eq. (9.151), the cutoff at the air–film boundary is

$$\beta > n_0 k \tag{9.154}$$

Whereas from Eq. (9.152), the cutoff at the film–substrate boundary is

$$\beta > n_2 k \tag{9.155}$$

Since n_2 is larger than n_0, if Eq. (9.155) is satisfied, Eq. (9.154) is automatically satisfied. Thus, for transmission, β must satisfy the condition

$$n_1 k > \beta > n_2 k \tag{9.156}$$

This is a narrow region fenced in by the hatched sections in Fig. 9.15a.

Next, an approximate expression for the characteristic equation is found. The difference in the refractive indices $n_1 - n_0$ is much larger than that of $n_2 - n_1$ and the following approximation is possible. Since the range of β where mode propagation takes place is so narrow, the value of γ_0 can be assumed constant over this range (see the curve of γ_0 in Fig. 9.15a). Moreover, γ_0 in this region is much larger than $K_{\max}$. Hence, the value of $\delta_{\parallel}^{c} = \tan^{-1}(\gamma_0 / n_0'^2 K)$ ranges from 70° to 90° depending on the value of K. For simplicity, $\delta_{\parallel}^{c} \doteqdot \pi/2$ is assumed for the time being. With this assumption, Eq. (9.146) is simplified:

$$-\cot 2Kd = \frac{\gamma_2}{n_2'^2 K} \tag{9.157}$$

It is interesting to note that Eq. (9.157) is similar to the characteristic equation [Eq. (9.31)] for the odd TM modes inside the symmetric guide, but with a factor of 2.

Another relationship has to be found to solve for K and γ_2. From Eqs. (9.150) and (9.152), we have

$$(\gamma_2 d)^2 + (Kd)^2 = V_2^2 \tag{9.158}$$

where

$$V_2 = kd\sqrt{n_1^2 - n_2^2} \tag{9.159}$$

Equations (9.157) and (9.158) are plotted in Fig. 9.16 to find the solutions. Now, we are ready to answer the questions.

(a) From Fig. 9.16, starting with $V_2 = \pi/4$, new modes are generated at an interval of $\pi/2$ radians. Modes up to the μth mode are excited if

$$\frac{\pi}{4} < V_2 < \frac{\pi}{4} + \frac{\pi}{2}(\mu + 1) \tag{9.160}$$

If μ is the largest integer that satisfies Eq. (9.160), then the number of possible modes is $\mu + 1$.

(b) The single-mode condition is again, from Fig. 9.16,

$$\frac{\pi}{4} < V_2 < \frac{3\pi}{4}$$

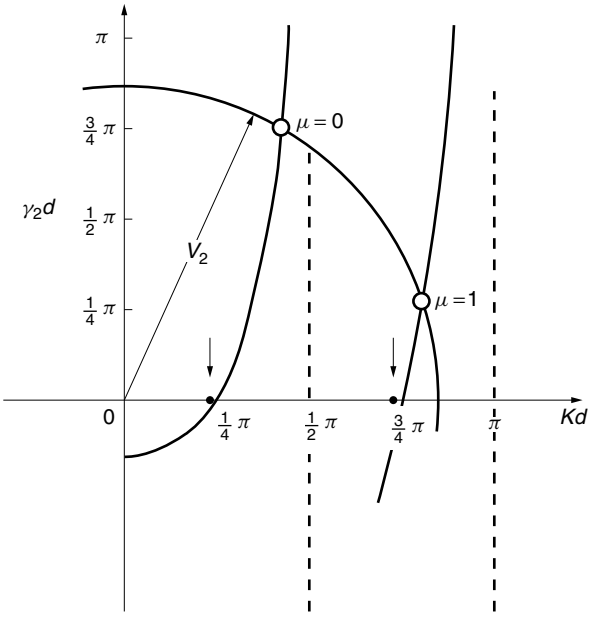

Figure 9.16 Graphical solutions for the asymmetrical guide. The exact locations of the intersections determined by the numerical methods are slightly to the left, as indicated by the arrows.

or the thickness $2d$ of the film has to satisfy

$$\frac{0.25\lambda}{\sqrt{n_1^2 - n_2^2}} < 2d < \frac{0.75\lambda}{\sqrt{n_1^2 - n_2^2}} \tag{9.161}$$

An important feature of the asymmetric guide is that, unlike the symmetric guide, the lowest order mode does have a cutoff and this cutoff occurs near $V_2 = \pi/4$.

(c) The distribution of the H_y field in the core will be found using Eq. (9.74). In the air layer, only the evanescent wave exists. Inserting Eqs. (9.74) and (9.75) into Eqs. (9.82) and (9.86), with $x = 0$, gives

$$\frac{B}{A} = \frac{Z_0}{Z_1}$$

The values of Z_0 and Z_1 are given by Eqs. (9.102) and (9.126) and

$$\frac{B}{A} = \frac{\gamma_0}{n_0'^2 K} \tag{9.162}$$

As we already found from the curves in Fig. 9.15, the right-hand side of Eq. (9.162) is very large. Hence, B is much larger than A and the distribution function of Eq. (9.74) can be approximated as

$$H_y = B \sin Kx \tag{9.163}$$

The value of K for the zero-order mode is, from Fig. 9.16,

$$\frac{\pi}{4d} < K < \frac{\pi}{2d}$$

The distribution of H_y with $\mu = 0$ is shown in Fig. 9.15b together with higher order modes.

(d) In the region

$$0 < \beta < n_0 k \tag{9.164}$$

total internal reflection does not take place at either interface and the light ray penetrates these boundaries according to the usual laws of reflection and refraction at boundaries.

We next examine the region

$$n_0 k < \beta < n_2 k \tag{9.165}$$

When β satisfies this condition, total internal reflection does not take place at the film–substrate interface, but the light is totally internally reflected at the air–film interface.

In the region

$$n_2 k < \beta < n_1 k - \epsilon \tag{9.166}$$

guided modes exist. The small number ϵ (shown in the expanded graph on the right side of Fig. 9.15a) is introduced to account for the fact that K in $\beta = \sqrt{(n_1 k)^2 - K^2}$ does not become $n_1 k$ because the lowest mode is cut off at $Kd = \pi/4$ and not at $Kd = 0$.

Ray paths of these regions are summarized in Fig. 9.15c. □

9.9 COUPLED GUIDES

Coupling between optical guides can be treated as a five-layer medium problem. Such a five-layer medium consists of two guiding layers with higher index of refraction, spaced by a center layer with lower index of refraction.

9.9.1 Characteristic Equations of the Coupled Slab Guide

Now, let us start with the calculation of the propagation constants of the coupled slab guide. The refractive index distribution is shown in Fig. 9.17. For simplicity, the distribution was chosen to be symmetric with respect to $x = 0$. The geometry is the same as the W guide explained in Example 9.5. The only difference is that this time there is a refractive index ditch in the center, and the d_2 layers in Fig. 9.11 become the guiding layers. The analysis procedures are quite similar and only a brief outline will be repeated here.

Because of the symmetry in the geometry, the product $[T_-]$ of the transmission matrices for the bottom half of the layers suffice. The layers in the bottom half are

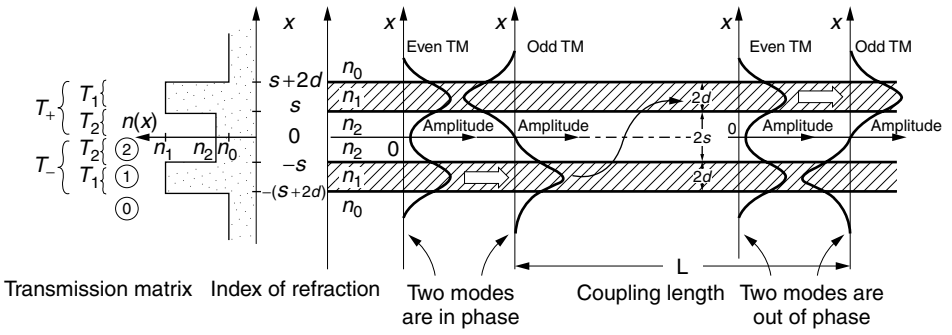

Figure 9.17 Slab optical coupler with symmetry in the refractive index distribution.

designated as

$$\begin{aligned} &\text{Region 2} \quad -s < x < 0 \\ &\text{Region 1} \quad -(s+2d) < x < -s \\ &\text{Region 0} \quad x < -(s+2d) \end{aligned} \tag{9.167}$$

The $[T_-]$ transfers

$$\begin{bmatrix} H_y(0) \\ E_z(0) \end{bmatrix} = [T_-] \begin{bmatrix} H_y(-(s+2d)) \\ E_z(-(s+2d)) \end{bmatrix} \tag{9.168}$$

where

$$[T_-] = [T_2][T_1] \tag{9.169}$$

and where $[T_1]$ and $[T_2]$ are transmission matrices for regions 1 and 2. For the mode that has the evanescent wave in region 2 and guided wave in region 1, $[T_-]$ becomes

$$T_- = \begin{bmatrix} \cosh \gamma_2 s & \dfrac{1}{Z_2} \sinh \gamma_2 s \\ Z_2 \sinh \gamma_2 s & \cosh \gamma_2 s \end{bmatrix} \begin{bmatrix} \cos 2K_1 d & \dfrac{1}{Z_1} \sin 2K_1 d \\ -Z_1 \sin 2K_1 d & \cos 2K_1 d \end{bmatrix} \tag{9.170}$$

If we put $[T_-]$ as

$$[T_-] = \begin{bmatrix} A & B \\ C & D \end{bmatrix} \tag{9.171}$$

then, as explained in Section 9.7.3, the characteristic equations for the even and odd modes are

$$C + Z_0 D = 0 \quad \text{even mode} \tag{9.172}$$

$$A + Z_0 B = 0 \quad \text{odd mode} \tag{9.173}$$

where

$$Z_0 = \frac{j\gamma_0}{\omega\epsilon_0 n_0^2}$$
$$Z_1 = \frac{jK_1}{\omega\epsilon_0 n_1^2} \tag{9.174}$$
$$Z_2 = \frac{j\gamma_2}{\omega\epsilon_0 n_2^2}$$

From Eqs. (9.170) to (9.172), the characteristic equation for the even modes becomes

$$\begin{aligned} &-\frac{\gamma_2}{n_2^2}\tanh\,\gamma_2 s + \frac{K_1}{n_1^2}\tan 2K_1 d \\ &-\frac{\gamma_0}{n_0^2}\left[1 + \frac{\gamma_2}{K_1}\left(\frac{n_1}{n_2}\right)^2 \tanh\,\gamma_2 s \tan 2K_1 d\right] = 0 \end{aligned} \tag{9.175}$$

Similarly, the characteristic equation for the odd modes becomes

$$\begin{aligned} &1 - \frac{K_1}{\gamma_2}\left(\frac{n_2}{n_1}\right)^2 \tanh\,\gamma_2 s \tan 2K_1 d + \frac{\gamma_0}{K_1}\left(\frac{n_1}{n_0}\right)^2 \tan 2K_1 d \\ &+ \frac{\gamma_0}{\gamma_2}\left(\frac{n_2}{n_0}\right)^2 \tanh\,\gamma_2 s = 0 \end{aligned} \tag{9.176}$$

The equations for the attenuation and propagation constants are

$$\gamma_0^2 = \beta^2 - (n_0 k)^2 \tag{9.177}$$
$$K_1^2 = (n_1 k)^2 - \beta^2 \tag{9.178}$$
$$\gamma_2^2 = \beta^2 - (n_2 k)^2 \tag{9.179}$$

The equations for the normalized thicknesses are

$$V_0^2 = (K_1 d)^2 + (\gamma_0 d)^2 \tag{9.180}$$
$$V_2^2 = (K_1 d)^2 + (\gamma_2 d)^2 \tag{9.181}$$
$$V_0 = kd\sqrt{n_1^2 - n_0^2} \tag{9.182}$$
$$V_2 = kd\sqrt{n_1^2 - n_2^2} \tag{9.183}$$

Equations (9.175) and (9.176) can be rewritten in a form similar to Eq. (9.131). The curves of $\gamma_0 d$ versus $K_1 d$ of either Eq. (9.175) or (9.176) are made incorporating Eq. (9.181). The intersections of the characteristic equation with the circle of Eq. (9.180) are the solutions for the K_{1x} even and the K_{1x} odd modes.

From the solutions for the K_{1x} even and K_{1x} odd modes, β_e and β_0 are found as

$$\beta_e = \sqrt{(n_1 k)^2 - K_{1x\,\text{even}}^2} \tag{9.184}$$

$$\beta_0 = \sqrt{(n_1 k)^2 - K_{1x\,\text{odd}}^2} \tag{9.185}$$

An actual calculation will be given in Example 9.7.

9.9.2 Amplitude Distribution in the Coupled Slab Guide

Next, the amplitude distribution across the five layers will be calculated. Only the case of the lowest order mode is treated and the subscript indicating the mode order will be suppressed. The field in the center region is calculated first, and then the outer regions in the order of 2, 1, and lastly 0.

Let us begin with the field of the even mode. The boundary field of the even mode in the $x = 0$ plane is $E_z(0) = 0$ as explained earlier in Section 9.7.3. Note that the transmission matrix is always used from the bottom to the top in each region. Only the field in the bottom half group of layers will be considered.

Field in Region 2 The field inside region 2, which extends from $x = -s$ to 0, is, from Eq. (9.98),

$$\begin{bmatrix} H_{y2}(x) \\ E_{z2}(x) \end{bmatrix} = \begin{bmatrix} \cosh\,\gamma_2(x+s) & \dfrac{1}{Z_2}\sinh\,\gamma_2(x+s) \\ Z_2\,\sinh\,\gamma_2(x+s) & \cosh\,\gamma_2(x+s) \end{bmatrix} \begin{bmatrix} H_{y2}(-s) \\ E_{z2}(-s) \end{bmatrix} \tag{9.186}$$

where $0 > x > -s$. Since we are dealing with the even mode, the condition of $E_{z2}(0) = 0$ as in Eq. (9.116) is used to simplify Eq. (9.186). From the bottom row of Eq. (9.186) with $x = 0$,

$$E_{z2}(-s) = -Z_2 H_{y2}(-s)\,\tanh\,\gamma_2 s \tag{9.187}$$

Insertion of Eq. (9.187) into the top row of Eq. (9.186) gives

$$H_{y2}(x) = \frac{\cosh\,\gamma_2 x}{\cosh\,\gamma_2 s} H_{y2}(-s)$$

and

$$H_{y2}(0) = H(0) = \frac{1}{\cosh\,\gamma_2 s} H_{y2}(-s) \tag{9.188}$$

From Eqs. (9.187) through (9.189), we have

$$H_{y2}(x) = H(0)\,\cosh\,\gamma_2 x \tag{9.189}$$

Insertion of Eq. (9.187) into the bottom row of Eq. (9.186) and the use of Eq. (9.188) give

$$E_{z2}(x) = H(0) Z_2\,\sinh\,\gamma_2 x \tag{9.190}$$

Field in Region 1 The field in region 1 is given by Eq. (9.80):

$$\begin{bmatrix} H_{y1}(x) \\ E_{z1}(x) \end{bmatrix} = \begin{bmatrix} \cos K_1(x+s+2d) & \dfrac{1}{Z_1}\sin K_1(x+s+2d) \\ -Z_1 \sin K_1(x+s+2d) & \cos K_1(x+s+2d) \end{bmatrix} \begin{bmatrix} H_{y1}(-(s+2d)) \\ E_{z1}(-(s+2d)) \end{bmatrix} \tag{9.191}$$

where

$$-s < x < -(s+2d)$$

The fields at the top of region 1 have to match those of the bottom of Region 2:

$$\begin{aligned} H_{y1}(-s) &= H_{y2}(-s) = H(0)\cosh \gamma_2 s \\ E_{z1}(-s) &= E_{z2}(-s) = -H(0)Z_2 \sinh \gamma_2 s \end{aligned} \tag{9.192}$$

where use was made of Eqs. (9.189) and (9.190).

Removing $H(0)$ from Eq. (9.192), we have

$$E_{z1}(-s) = -Z_2 H_{y1}(-s) \tanh \gamma_2 s \tag{9.193}$$

Inserting the boundary condition into Eq. (9.191) with $x = -s$ gives

$$\begin{bmatrix} H_{y1}(-s) \\ -Z_2 H_{y1}(-s) \tanh \gamma_2 s \end{bmatrix} = \begin{bmatrix} \cos 2K_1 d & \dfrac{1}{Z_1}\sin 2K_1 d \\ -Z_1 \sin 2K_1 d & \cos 2K_1 d \end{bmatrix} \begin{bmatrix} H_{y1}(-(s+2d)) \\ E_{z1}(-(s+2d)) \end{bmatrix} \tag{9.194}$$

Equation (9.194) will be inverted so that

$$\begin{bmatrix} H_{y1}(-(s+2d)) \\ E_{z1}(-(s+2d)) \end{bmatrix}$$

is used in Eq. (9.191). Recall that the matrix inversion is

$$\begin{bmatrix} a & b \\ c & d \end{bmatrix}^{-1} = \frac{1}{\Delta}\begin{bmatrix} d & -b \\ -c & a \end{bmatrix} \tag{9.195}$$

After inserting Eq. (9.192), Eq. (9.194) is inverted using Eq. (9.195) to obtain

$$\begin{bmatrix} H_{y1}(-(s+2d)) \\ E_{z1}(-(s+2d)) \end{bmatrix} = \begin{bmatrix} H(0)\cos 2K_1 d \cosh \gamma_2 s + H(0)\dfrac{Z_2}{Z_1}\sin 2K_1 d \sinh \gamma_2 s \\ H(0)Z_1 \sin 2K_1 d \cosh \gamma_2 s - H(0)Z_2 \cos 2K_1 d \sinh \gamma_2 s \end{bmatrix} \tag{9.196}$$

Inserting Eq. (9.196) into (9.191) gives

$$H_{y1}(x) = H(0)\left[\cos K_1(x+s) - \frac{Z_2}{Z_1}\sin K_1(x+s)\tanh \gamma_2 s\right]\cosh \gamma_2 s \tag{9.197}$$

$$E_{z1}(x) = -H(0)Z_1\left[\sin K_1(x+s) + \frac{Z_2}{Z_1}\cos K_1(x+s)\tanh \gamma_2 s\right]\cosh \gamma_2 s \tag{9.198}$$

Field in Region 0 In region 0, both $H_{y0}(x)$ and $E_{z0}(x)$ decay exponentially and the relationship between them is $E_{z0}(x) = Z_0 H_{y0}(x)$ as seen from Eq. (9.82). The fields at the top of region 0 have to be *smoothly* connected with $H_{y1}(-(s+2d))$ and $E_{z1}(-(s+2d))$ in region 1. The fields are

$$H_{y0}(x) = H(0)\left[\cos 2K_1 d + \frac{Z_2}{Z_1}\sin 2K_1 d \tanh \gamma_2 s\right] \cosh \gamma_2 s(e^{\gamma_0(x+s+2d)}) \tag{9.199}$$

$$E_{z0}(x) = H(0)\left[Z_1 \sin 2K_1 d - Z_2 \cos 2K_1 d \tanh \gamma_2 s\right] \cosh \gamma_2 s(e^{\gamma_0(x+s+2d)}) \tag{9.200}$$

Table 9.1 Even TM modes in the coupled slab guide

Even TM Mode Fields			
Region	x	$H_y(x)$	$E_z(x)$
0	$s+2d$	$Ce^{-\gamma_0(x-s-2d)}$	$-Z_0 Ce^{-\gamma_0(x-s-2d)}$
1	s	$A\cos K_1(x-s) + B\sin K_1(x-s)$	$Z_1[-A\sin K_1(x-s) + B\cos K_1(x-s)]$
2	0	$H(0)\cosh \gamma_2 x$	$Z_2 H(0)\sinh \gamma_2 x$
1	$-s$	$A\cos K_1(x+s) - B\sin K_1(x+s)$	$-Z_1[A\sin K_1(x+s) + B\cos K_1(x+s)]$
0	$-s-2d$	$Ce^{\gamma_0(x+s+2d)}$	$Z_0 Ce^{\gamma_0(x+s+2d)}$

$A = H(0)\cosh \gamma_2 s$

$B = H(0)\dfrac{Z_2}{Z_1}\sinh \gamma_2 s$

$C = H(0)[\cos 2K_1 d \cosh \gamma_2 s + \dfrac{Z_2}{Z_1}\sin 2K_1 d \sinh \gamma_2 s]$

Table 9.2 Odd TM modes in the coupled slab guide

Odd TM Mode Fields			
Region	x	$H_y(x)$	$E_z(x)$
0	$s+2d$	$-C'e^{-\gamma_0(x-s-2d)}$	$Z_0 C'e^{-\gamma_0(x-s-2d)}$
1	s	$A'\cos K_1(x-s) - B'\sin K_1(x-s)$	$Z_1[A'\sin K_1(x-s) - B'\cos K_1(x-s)]$
2	0	$-H(0)\sinh \gamma_2 x$	$-Z_2 H(0)\cosh \gamma_2 x$
1	$-s$	$-A'\cos K_1(x+s) - B'\sin K_1(x+s)$	$Z_1[-A'\sin K_1(x+s) - B'\cos K_1(x+s)]$
0	$-s-2d$	$C'e^{\gamma_0(x+s+2d)}$	$Z_0 C'e^{\gamma_0(x+s+2d)}$

$A' = H(0)\sinh \gamma_2 s$

$B' = H(0)\dfrac{Z_2}{Z_1}\cosh \gamma_2 s$

$C' = H(0)[\cosh 2K_1 d \sinh \gamma_2 s + \dfrac{Z_2}{Z_1}\sin 2K_1 d \cosh \gamma_2 s]$

The smoothness of the connection is enforced by the characteristic equation, Eq. (9.172), which was originally derived from the smooth connection of both H_y and its derivative. With this condition, the ratio between the terms in square brackets in Eqs. (9.199) and (9.200) is found to be Z_0 (see Problem 9.8).

The amplitude distributions of the even TM modes in the coupled slab guide are tabulated in Table 9.1. The same for the odd TM modes are tabulated in Table 9.2.

Example 9.7 Using a lithium niobate substrate, coupled slab guides were fabricated. The dimensions and refractive indices are indicated in Fig. 9.18.

(a) Find the propagation constants of the first even and odd modes.
(b) Find the expression for the fields H_y and E_z of the even and odd modes, of the lowest order with respect to x. Draw the curve for $H_y(x)$.

Solution

(a) A slightly different approach will be taken to calculate the numerical solutions. So far, the mode values have been obtained from the intersections between the characteristic equation and the circle of the normalized thickness. The intersections provided the values of both K_d and γ_d at the same time.

Let us put the left-hand side of Eq. (9.175) as $f(K_1 d)$. Every term in Eq. (9.175) can be expressed in terms of $K_1 d$ using Eqs. (9.180) to (9.183). The function $f(K_1 d)$ is plotted with respect to $K_1 d$. Figure 9.19 shows such a graph. The intersections of $f(K_1 d)$ with the $K_1 d$ axis are the solutions for $K_1 d$. This method provides the solutions only for $K_1 d$, but is straightforward.

$$\begin{aligned} K_{1x\text{even}} d &= 1.1939 \\ K_{1x\text{odd}} d &= 1.1955 \end{aligned} \tag{9.201}$$

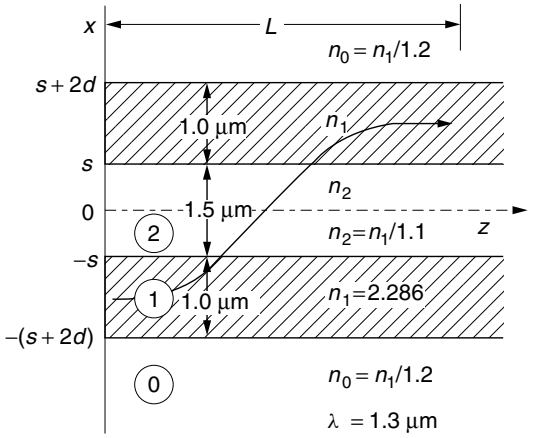

Figure 9.18 Geometry and dimensions of coupled slab guides.

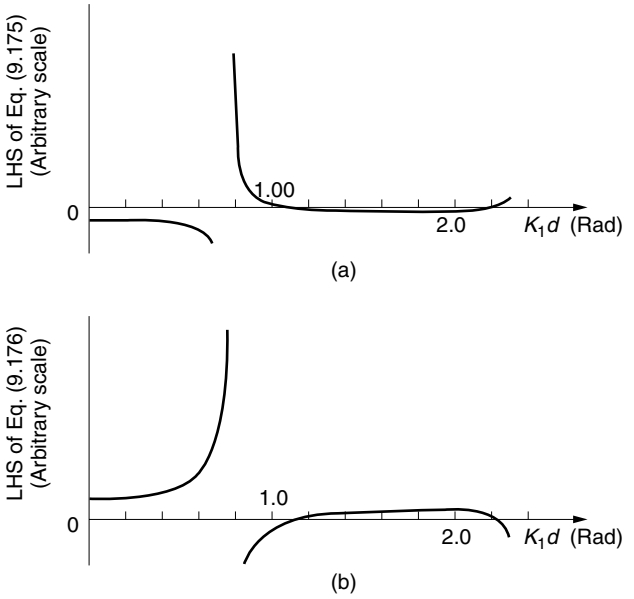

Figure 9.19 Solutions of the characteristic equations. (a) Solution for even-order modes. (b) Solution for odd-order modes. (Calculation courtesy of R. James.)

From Eq. (9.178), β_e and β_0 are calculated as

$$\begin{aligned} \beta_e &= 10.788\ \mu\text{m}^{-1} \\ \beta_0 &= 10.787\ \mu\text{m}^{-1} \end{aligned} \tag{9.202}$$

(b) In order to use the formulas in Table 9.1, γ_0, γ_2, and K_1 are calculated using Eqs. (9.180), (9.181), and (9.201).

	Even Mode	Odd Mode
γ_0 (μm^{-1})	5.6213	5.6199
K_1 (μm^{-1})	2.3877	2.3910
γ_2 (μm^{-1})	3.9351	3.9331

$$\begin{aligned} s &= 0.75\ \mu\text{m} \\ d &= 0.50\ \mu\text{m} \\ \lambda &= 1.3\ \mu\text{m} \\ n_1 &= 2.286 \\ n_0 &= n_1/1.2 \\ n_2 &= n_1/1.1 \end{aligned}$$

Figure 9.20 shows the field distribution of the even and odd TM modes calculated using the parameters and geometries shown in Fig. 9.18. □

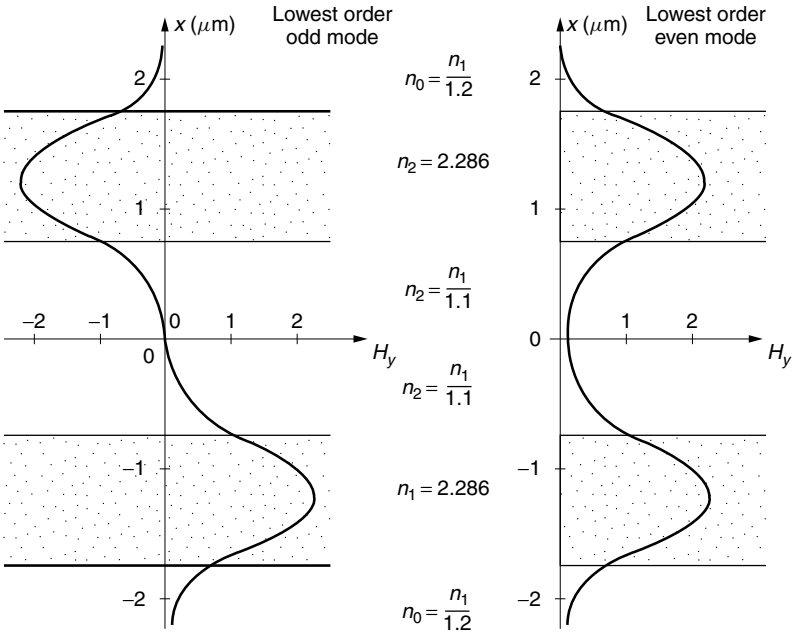

Figure 9.20 Calculation of the field $H_y(x)$ along the x axis inside the five-layer medium. (Calculation courtesy of R. James.)

9.9.3 Coupling Mechanism of the Slab Guide Coupler

We are now able to discuss the coupling mechanism of the slab guide coupler [8]. Figure 9.17 shows the cross section of a five-layer medium that forms a coupled slab guide. The coupling mechanism is interpreted from the change in the relative phase of the fundamental odd and even modes. As shown in Fig. 9.20, the field distribution of the even mode has two symmetric humps along the x axis, while that of the odd mode has two antisymmetric humps along the x direction. With the presence of the even and odd modes of equal amplitude, the two fields enhance each other and the resultant amplitude is nearly doubled in the lower guides in Fig. 9.17, whereas inside the upper guide, the two fields nearly cancel each other and the amplitude is almost null. With this distribution of the resultant fields, it appears as if only the lower guide is excited.

Because of the difference in the propagation constants of the even and odd modes, after some distance of propagation, the relative phase between the even and odd modes becomes 180°, so that the resultant field in the upper guide becomes large whereas the resultant field in the lower guide becomes null. The resultant field intensities in the upper and lower guides reverse. This is interpreted as the transfer of the light energy from the lower to the upper guide. The length of the transfer of the energy is called the *transfer length*. After another transfer length, the light energy returns to the lower guide. Light goes back and forth between the guides.

The transfer length L is given from Eqs. (9.184) and (9.185) by

$$L = \frac{\pi}{\beta_e - \beta_o} \tag{9.203}$$

The value of L with Example 9.7 is 4.41 mm.

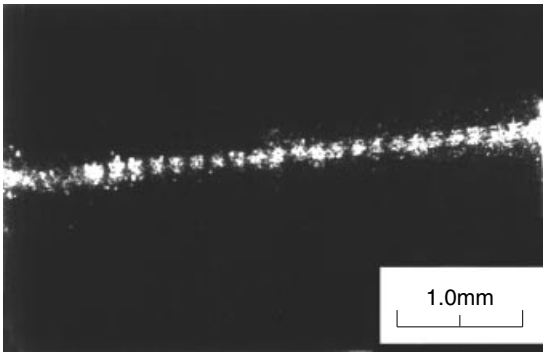

Figure 9.21 Fields seen from the top surface of the coupled slab guides. The film records light scattered from the top guiding layer. (Courtesy of N. Goto, Y. Miyazaki, and Y. Akao [9].)

The relative field strengths between the guides at a distance other than the transfer length are obtained by adding the even- and odd-mode fields with the relative phase taken into consideration.

Figure 9.21 is a photograph taken looking downward on the top surface of a five-layer medium [9]. The light is transferred back and forth between the two guiding layers. The film records only the light scattered from the upper guide layer, and the photograph shows a sequence of dots of light.

PROBLEMS

9.1 Why is only one quadrant drawn in Fig. 9.2?

9.2 Obtain the angle of propagation of the component plane waves of the highest order TM mode when the normalized thickness V is a multiple of $\pi/2$ radians.

9.3 What is the range of thickness $2d$ of a slab optical guide that has a *total* of five *possible* TM modes, where $\lambda = 0.85$ μm, $n_1 = 1.55$, and $n_2 = 1.54$.

9.4 Choose either *increase* or *decrease* in the following sentences. If the thickness of the slab guide is *decreased* with all other physical constants fixed, the normalized thickness V (*increases, decreases*) and $K_2 d$ of the TM_2 mode (*increases, decreases*) and the value of K_2 (*increases, decreases*), and this means that the value of β_2 (*increases, decreases*). Thus, in order to obtain a region of larger effective index of refraction $N = \beta_2/k$, the thickness $2d$ has to be (*increased, decreased*).

9.5 With a symmetric slab guide such as shown in Fig. P9.5, the cross-sectional distribution of the light intensity was examined. It was found that among the K values, the largest $K_{\max}$ was

$$K_{\max} = 1.0 \text{ rad}/\mu\text{m}$$

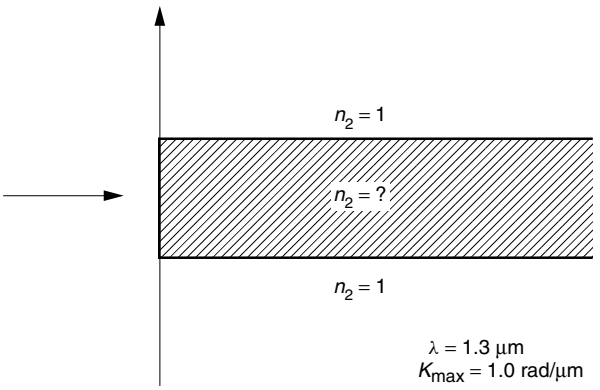

Figure P9.5 Symmetric optical guide with unknown refractive index of the core layer.

Find the index of refraction n_1 of the core layer. The index of refraction n_2 of the cladding is unity and the wavelength of the light is 1.3 μm.

9.6 An slab optical guide is bent as shown in Fig. P9.6. Find the radius of curvature r of bending that will start leaking light into the cladding for these parameters:

$$\Delta = (n_1 - n_2)/n_1 = 0.055$$

$$d = 50 \text{ μm}$$

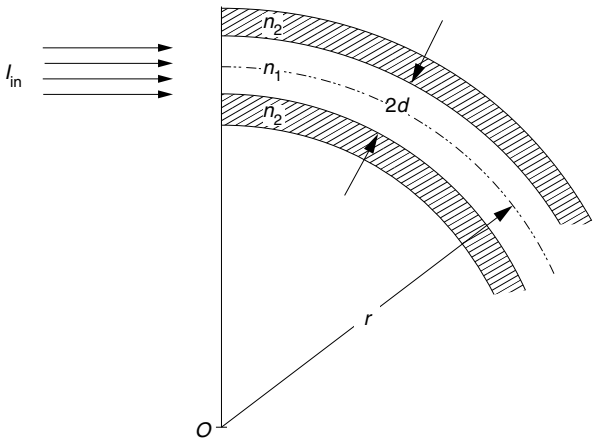

Figure P9.6 Leak from a bent optical guide.

9.7 Find the characteristic equation of an asymmetric guide with the geometry shown in Fig. P9.7, using (a) the coefficient matrix method and (b) the transmission matrix method. Compare the results. The TM wave is excited.

9.8 Verify that the ratio $E_{z0}(x)/H_{y0}(x)$ of Eqs. (9.199) and (9.200) is equal to Z_0.

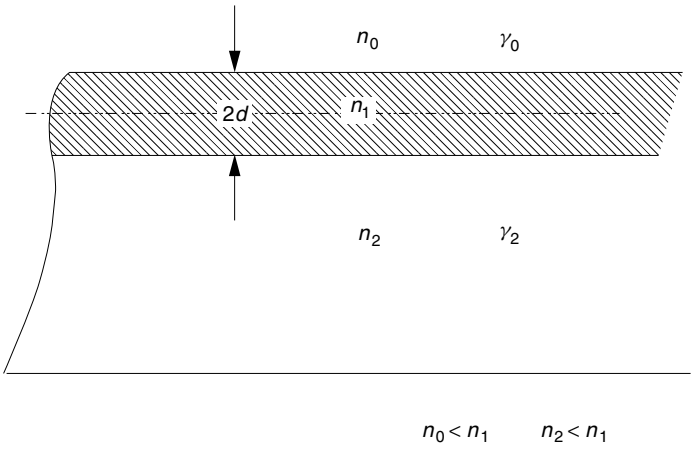

Figure P9.7 Geometry of an asymmetric guide.

REFERENCES

1. R. G. Hunsperger, *Integrated Optics: Theory and Technology*, 4th ed., Springer-Verlag, Berlin, 1995.
2. B. E. A. Saleh and M. C. Teich, *Fundamentals of Photonics*, Wiley, New York, 1991.
3. T. Tamir (ed.), *Guided-Wave Optoelectronics*, Springer-Verlag, Berlin, 1990.
4. A. R. Mickelson, *Guided Wave Optics*, Van Nostrand Reinhold, New York, 1993.
5. K. Iizuka, *Engineering Optics*, 2nd ed., Springer-Verlag, Berlin, 1987.
6. Y. Suematsu and K. Furuya, "Propagation mode and scattering loss of a two-dimensional dielectric waveguide with gradual distribution of refractive index," *IEEE Trans. Microwave Theory and Tech.* **MTT-20**(8), 524–531 (1972).
7. Y. Mushiake and M. Kudo, "Multilayered optical slab guide," in *Optical Guided-Wave Electronics*, by the Editorial Committee of the Special Project Research on Optical Guided-Wave Electronics of Japan, Tokyo, 1981, pp. 17–37.
8. A. B. Buckman, *Guided-Wave Photonics*, Saunders College Publishing, Austin, TX, 1992.
9. N. Goto, Y. Miyazaki, and Y. Akao, "Tunable filtering characteristics of multilayered optical couplers using surface acoustic waves," *Japanese Journal of Applied Physics*, **21**(11), 1611–1615 (1982).